

AD-A100 885

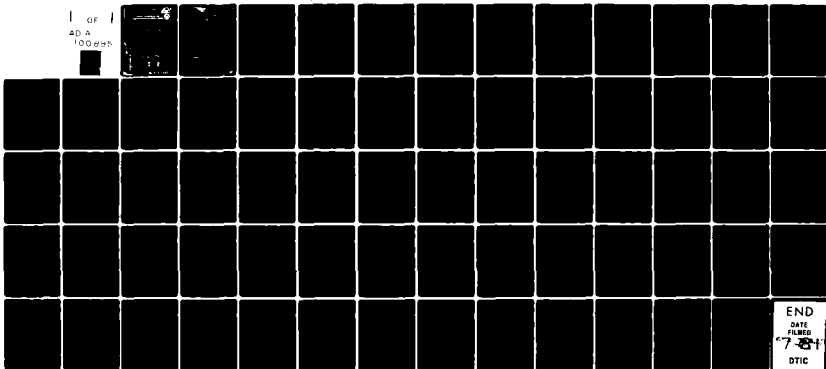
DAVID W TAYLOR NAVAL SHIP RESEARCH AND DEVELOPMENT CE--ETC F/6 20/4  
CALCULATION OF NATURAL VIBRATION FREQUENCIES AND TRANSIENT RESP--ETC(U)  
JUN 81 R V RAETZ, G C EVERSTINE

UNCLASSIFIED

DTNSRDC-81/051

NL

1 OF 1  
40 A  
100885

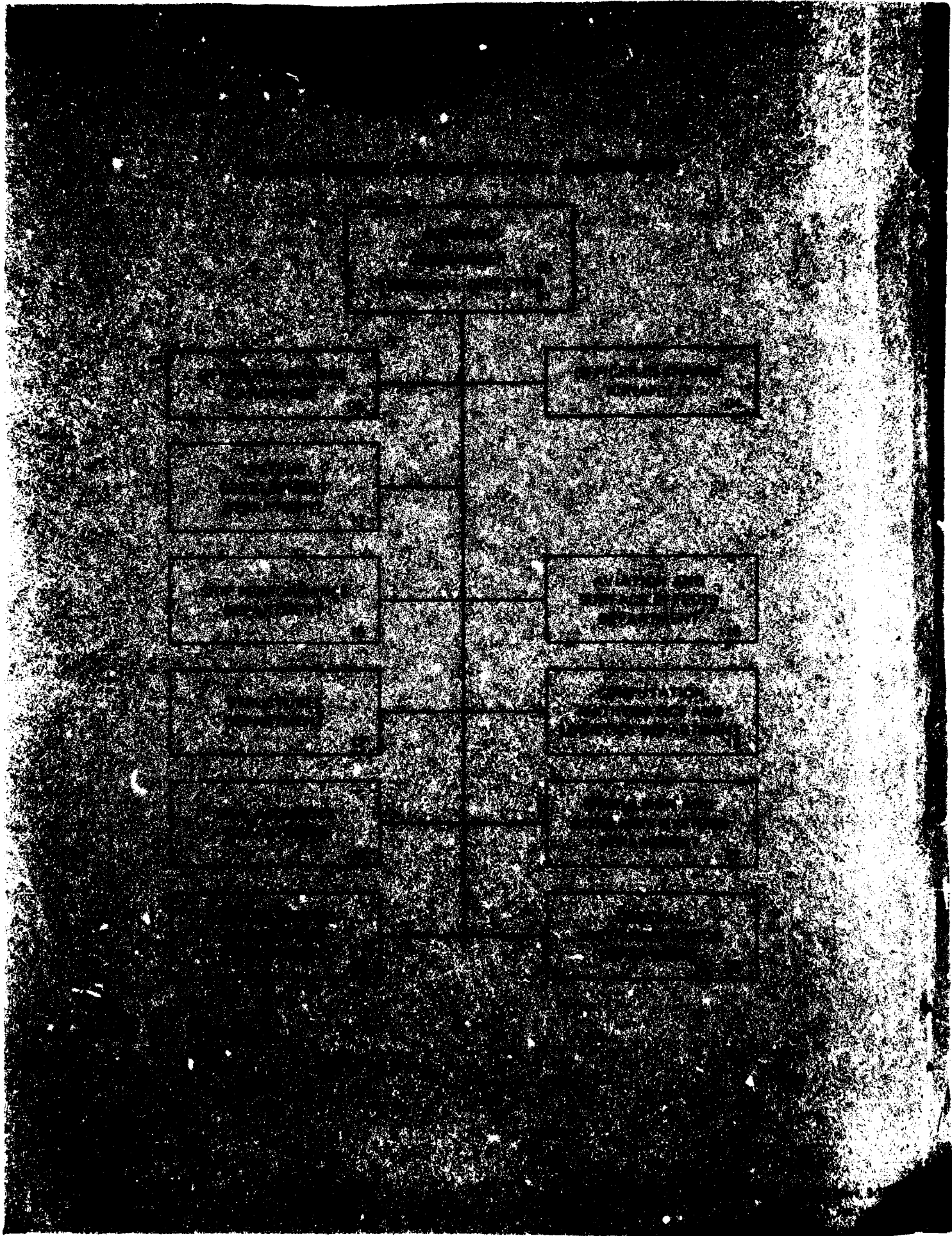


END  
DATE  
7-28-81  
OTIC

AD A 7 1

OPTION

OPTION



UNCLASSIFIED

SECURITY CLASSIFICATION OF THIS PAGE (When Data Entered)

17/1/73-1-1861

REPORT DOCUMENTATION PAGE		READ INSTRUCTIONS BEFORE COMPLETING FORM
1. REPORT NUMBER DTNSRDC-81/051	2. GOVT ACCESSION NO. AD A100885	3. RECIPIENT'S CATALOG NUMBER (1)
4. TITLE (and Subtitle) CALCULATION OF NATURAL VIBRATION FREQUENCIES AND TRANSIENT RESPONSE OF PARTIALLY SUBMERGED, SUPERCAVITATING MARINE PROPELLERS		5. TYPE OF REPORT & PERIOD COVERED Final report
6. AUTHOR(s) Richard V. Raetz Gordon C. Everstine		7. CONTRACT OR GRANT NUMBER(s)
8. PERFORMING ORGANIZATION NAME AND ADDRESS David W. Taylor Naval Ship Research and Development Center Bethesda, Maryland 20084		9. PROGRAM ELEMENT, PROJECT, TASK AREA & WORK UNIT NUMBERS (See reverse side)
10. CONTROLLING OFFICE NAME AND ADDRESS Naval Sea Systems Command Washington, D.C. 20362		11. REPORT DATE Jun 1981
12. MONITORING AGENCY NAME & ADDRESS (if different from Controlling Office) 12/65		13. NUMBER OF PAGES 64
14. DISTRIBUTION STATEMENT (of this Report)		15. SECURITY CLASS. (of this report) UNCLASSIFIED
16. DISTRIBUTION STATEMENT (of the abstract entered in Block 20, if different from Report)		15a. DECLASSIFICATION/DOWNGRADING SCHEDULE
17. SUPPLEMENTARY NOTES		
18. KEY WORDS (Continue on reverse side if necessary and identify by block number) Propellers Fluid-Structure Interaction Propeller Dynamic Response NASTRAN- DMAP Application Propeller Vibration		
19. ABSTRACT (Continue on reverse side if necessary and identify by block number) Procedures are presented whereby natural vibration and transient response analyses of partially submerged, supercavitating marine propellers may be calculated by means of a standard NASTRAN structural analysis program. The use of these procedures was demonstrated by analyses of an existing propeller, for which some experimental data were available. Results were comparable only in a limited way, but peak calculated dynamic stresses were of		
(Continued on reverse side)		

UNCLASSIFIED

SECURITY CLASSIFICATION OF THIS PAGE (When Data Entered)

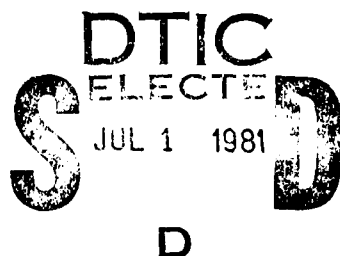
(Block 10)

Program Element 62543N  
Task Area ZP43-421-001  
Work Units 1500-200 and 1500-103

(Block 20 continued)

the same order of magnitude as those observed experimentally, and were apparently more than twice the magnitude of equivalent static stresses.

Accession For	
NTIS GRA&I	<input checked="" type="checkbox"/>
DTIC TAB	<input type="checkbox"/>
Unannounced	<input type="checkbox"/>
Justification	
By _____	
Distribution/ _____	
Availability Codes	
Dist	Avail and/or Special
R	



UNCLASSIFIED  
SECURITY CLASSIFICATION OF THIS PAGE (When Data Entered)

## TABLE OF CONTENTS

	Page
LIST OF FIGURES. . . . .	iii
LIST OF TABLES . . . . .	iv
ABSTRACT . . . . .	1
ADMINISTRATIVE INFORMATION . . . . .	1
INTRODUCTION . . . . .	1
DESCRIPTION OF ANALYSIS. . . . .	3
APPLICATION TO PROPELLER BLADES. . . . .	7
VIBRATION ANALYSIS OF P3604 PROPELLER. . . . .	15
TRANSIENT RESPONSE ANALYSIS OF SES-100B PROPELLER. . . . .	17
DISCUSSION OF SES-100B ANALYSIS RESULTS. . . . .	19
CONCLUSIONS. . . . .	23
ACKNOWLEDGMENTS. . . . .	24
APPENDIX - INPUT DATA PREPARATION. . . . .	39
REFERENCES . . . . .	57

## LIST OF FIGURES

1 - SES-100B Propeller Blade with Waterlines . . . . .	25
2 - Representation of Propeller Blade with Finite Elements . . . . .	26
3 - Finite Element Idealization of Propeller Blade . . . . .	27
4 - Representation of Fluid-Structure Contact Face of Water Mass with Finite Elements . . . . .	28
5 - Finite Element Idealization of Water Mass. . . . .	29
6 - Time-Dependent Blade Pressures . . . . .	30
7 - Calculated Radial Stress in Progressively Submerging Propeller Blade at Grid Point 22 . . . . .	31

	Page
8 - Calculated Radial Stress in Progressively Submerging Propeller Blade at Grid Point 36 . . . . .	32
9 - Calculated Radial Stress in Progressively Submerging Propeller Blade at Grid Point 39 . . . . .	33
10 - Calculated Radial Stress at Grid Point 22 of Propeller Blade in Air with Applied Dynamic Forces . . . . .	34
11 - Calculated Radial Stress at Grid Point 36 of Propeller Blade in Air with Applied Dynamic Forces . . . . .	35
12 - Calculated Radial Stress at Grid Point 39 of Propeller Blade in Air with Applied Dynamic Forces . . . . .	36
13 - Experimentally Determined Radial Stress in SES-100B Propeller Blade at Gage 1. . . . .	37
A.1 - Fluid Run Partial Input. . . . .	46
A.2 - Matrix PG of Equivalent Nodal Forces . . . . .	47
A.3 - Propeller Vibration Run Partial Input. . . . .	48
A.4 - Propeller Transient Response Run Input for Stage 1 . . . . .	49

#### LIST OF TABLES

1 - Calculated Natural Frequencies of P3604 Propeller Blade. . . . .	38
2 - Natural Frequencies of SES-100B Propeller Blade. . . . .	38

## ABSTRACT

Procedures are presented whereby natural vibration and transient response analyses of partially submerged, supercavitating marine propellers may be calculated by means of a standard NASTRAN structural analysis program. The use of these procedures was demonstrated by analyses of an existing propeller, for which some experimental data were available. Results were comparable only in a limited way, but peak calculated dynamic stresses were of the same order of magnitude as those observed experimentally, and were apparently more than twice the magnitude of equivalent static stresses.

## ADMINISTRATIVE INFORMATION

Funds for this investigation were obtained from the Naval Material Command (NAVMAT 0333) in support of an ongoing Ship Performance and Hydro-mechanics Exploratory Development Program (Program Element 62543N, Task Area ZP-43-421-001) assigned to the David W. Taylor Naval Ship Research and Development Center (DTNSRDC). The High Speed Propulsor Task of this Exploratory Development Program (DTNSRDC Work Unit No. 1500-200) provided funds to complete work presented in this report.

## INTRODUCTION

The utilization of high speed marine vehicles by the United States Navy has created a need for an improved structural analysis and design capability for high speed propulsors. These are generally supercavitating propellers, which may also be partially submerged. In their hydrodynamic performance and structural integrity, these propellers, because of their different geometries and modes of operation, represent substantial departure from conventional propellers, for which a large body of experience exists. Dynamic aspects of structural response, in particular, are expected to be more significant for these propellers. These aspects need to

be evaluated so that attempts to attain optimum hydrodynamic designs will not be limited unnecessarily by structural considerations. An effort was therefore instituted to develop methods of predicting dynamic stress and deflection behavior of high speed propellers under realistic time-dependent loading conditions.

A preliminary investigation indicated that meaningful results were not likely to be obtained other than by computer studies. Various computer programs have been used to calculate the full vibration modes and frequencies of completely submerged propellers, but until recently the effect of immersion in water has been accounted for by assuming that a more or less arbitrary mass of fluid is attached to the propeller blade. This "added effective mass" approach, which incorporates the assumption that the fluid is incompressible, is considered to account adequately for fluid structure interaction in most vibration and transient response problems, provided valid added fluid mass terms can be obtained. A few investigators have recently published descriptions of analyses of dynamic behavior of submerged structures in which effects of submergence in water are computed on a rational basis. One such investigation<sup>1\*</sup> yielded a procedure by which the existing NASTRAN finite element structural analysis program could be applied to the submerged structure problem, even without making the incompressibility assumption. That work forms the basis of the analyses described here. The approach was selected because of the availability of NASTRAN at DTNSRDC and because of its flexibility of application.

---

\*A complete listing of references is given on page 57.

Further modifications were made to this procedure to adapt it to the general problem of predicting free vibration frequencies and transient response of supercavitating, partially submerged propellers. The resulting approach was applied to determine natural frequencies of two propellers, and the dynamic stress response of one propeller for which some experimental data were available. Only a limited comparison of results was possible; however, the calculated frequencies and dynamic stresses appeared to be reasonable. The dynamic analysis and its application via NASTRAN are described in this report.

#### DESCRIPTION OF ANALYSIS

In the analysis to be used here, the fluid surrounding the submerged structure, in this case an individual propeller blade, is represented by a finite element idealization. More precisely, a quantity of fluid sufficiently large that its effect on the structure should nearly be the same as that of an infinite quantity is represented. The theory governing this approach is described by Zienkiewicz.<sup>2</sup> A concise presentation, with a delineation of the strategy of application by means of existing NASTRAN capabilities is given by Everstine et al.<sup>1</sup> The theory and application procedure will be briefly summarized here.

Conventional analytical techniques lead to the following matrix equation, which describes the dynamic behavior of the propeller blade when represented in finite element form:

$$[M]\{\ddot{u}\} + [K]\{u\} = \{F\} + [L]\{\bar{p}\} \quad (1)$$

where  $\{u\}$  is the set of unknown grid point displacements and  $\{F\}$  is a set of applied time-dependent forces. The column matrix  $\{\bar{p}\}$  is the set of unknown pressures on the fluid-structure interface grid points. The last term,  $[L]\{p\}$ , represents the fluid loading on the structure.

The set of unknown pressures at all the grid points of the fluid finite element idealization is represented in the following matrix equation:

$$[Q]\{\ddot{p}\} + [H]\{p\} = - [S]\bar{\{u\}} \quad (2)$$

The last term in Equation (2) represents the effect of accelerations of the structural grid points at the fluid structure interface on the pressures in the fluid. The bar placed over  $\{u\}$  indicates that only normal interface deflections are involved in that term. The fluid may be considered an acoustic medium, in which case Equation (2) provides a valid description of its dynamic behavior if it actually represents the wave equation

$$\nabla^2 p = \frac{1}{c^2} \ddot{p} \quad (3)$$

with appropriate boundary conditions. In Equation (3),  $c$  represents the speed of sound in the fluid. It was shown previously<sup>1</sup> that the implementation of the procedure can be accomplished by means of a standard structural program. The left side of Equation (2) is treated as being analogous to the left side of Equation (1), i.e., it is treated as a dynamics problem with unknown variables  $\{p\}$ . Only one translational degree of freedom at each grid point of the fluid is left unconstrained, however, and that one remaining component is interpreted as pressure. In addition, all degrees of freedom may be constrained on the outer fluid boundary (all boundary

points not in contact with the moveable structure). Finally for the three-dimensional case, the following material property matrix, representing Hooke's law, is used:

$$\left\{ \begin{array}{l} \sigma_{xx} \\ \sigma_{yy} \\ \sigma_{zz} \\ \sigma_{xy} \\ \sigma_{yz} \\ \sigma_{xz} \end{array} \right\} + \left[ \begin{array}{cccccc} 1 & -1 & -1 & 0 & 0 & 0 \\ -1 & 1 & -1 & 0 & 0 & 0 \\ -1 & -1 & 1 & 0 & 0 & 0 \\ 0 & 0 & 0 & 1 & 0 & 0 \\ 0 & 0 & 0 & 0 & 1 & 0 \\ 0 & 0 & 0 & 0 & 0 & 1 \end{array} \right] \left\{ \begin{array}{l} u_x \\ v_y \\ w_z \\ u_y + v_x \\ v_z + w_y \\ w_x + u_z \end{array} \right\} \quad (4)$$

With the NASTRAN program, it is not usually necessary to input the matrix (4). As pointed out by Everstine,<sup>3</sup> the same information can be input by specifying an isotropic material with the following values:

Shear modulus  $G = 1.0$

Poissons ratio  $\nu$  is not input (so the program will compute a value).

Young's modulus  $E = \alpha G$ ;  $\alpha \approx 1.0$

Here,  $\alpha + 1.0$  should be numerically indistinguishable from  $\alpha$ . On most computers,  $\alpha = 10^{20}$  will suffice. Equations (1) and (2) may now be combined into one set:

$$\left[ \begin{array}{cc} M & 0 \\ S & Q \end{array} \right] \left\{ \begin{array}{l} \ddot{u} \\ \ddot{p} \end{array} \right\} + \left[ \begin{array}{cc} K & -L \\ 0 & H \end{array} \right] \left\{ \begin{array}{l} u \\ p \end{array} \right\} = \left\{ \begin{array}{l} F \\ 0 \end{array} \right\} \quad (5)$$

A dynamic problem governed by Equation (5) can be run (the free vibration mode analysis results from letting  $F$  be null) by providing finite element data for both structure and fluid, in which case all matrices except

$S$  and  $L$  in Equation (5) will be set up automatically. Note that grid points for structure and fluid, including those on the interface which have the same coordinates, are numbered separately. Thus, the only coupling between fluid and structure is provided by the off-diagonal matrices,  $S$  and  $L$ . Equation (1), which expresses a balance of forces, shows that  $L$  relates the pressure at the fluid-structure interface to force resulting from that pressure. In a lumped formulation, the terms of  $L$  may be taken to be the interface surface areas associated with each fluid-structure interface grid point. In general, there will be three areas for each grid point - one for each coordinate direction. Zienkiewicz<sup>2</sup> has shown that

$$S = \rho L^T \quad (6)$$

Equation (5) then becomes

$$\begin{bmatrix} M & 0 \\ \rho L^T & Q \end{bmatrix} \begin{Bmatrix} \ddot{u} \\ \ddot{p} \end{Bmatrix} + \begin{bmatrix} K & -L \\ 0 & H \end{bmatrix} \begin{Bmatrix} u \\ p \end{Bmatrix} = \begin{Bmatrix} F \\ 0 \end{Bmatrix} \quad (7)$$

The  $L$  and  $L^T$  matrices may be determined separately and input directly, using the DMIG option of NASTRAN. Thus, formulation of Equation (7) (or Equation (5)) is completed, and the solution is carried out by the program. However, the presence of the off-diagonal matrices destroys the symmetry of the mass and stiffness matrices, requiring the use of time-consuming complex eigenvalue routines in the solution of these equations.

The natural vibration frequencies for some flat plates with varying levels of immersion were calculated by the method described and compared

with experimental results by Marcus.<sup>4</sup> Good agreement was obtained when a sufficient amount of water was modeled, and in fact the results provide a useful reference for judging the size of a fluid mass required to represent an infinite body of water.

#### APPLICATION TO PROPELLER BLADES

It was planned originally to apply the analysis as represented by Equation (7) to a supercavitating propeller blade, P3604, for which data for a finite element idealization were available from a previous stress study. The idealization consisted of 155 grid points and 16 quadratic isoparametric, twenty-noded, three-dimensional elements (NASTRAN data card CIHEx2). The purpose of this sample calculation was to verify that application of this procedure to the more complicated propeller blade would be feasible. It was apparent, however, that the cost of such a computer run could be high. A fluid idealization was constructed of only three layers of elements and extended one element beyond the edges of the blade. The fluid idealization, which was thought to be just large enough to represent an infinite quantity, but only on one side of the blade, contained 90 three-dimensional elements and 578 grid points. A total of 263 unconstrained degrees of freedom resulted, and this number would be about doubled for fluid on both sides of the blade. The blade itself was considered fixed along its base, so that a total of 396 degrees of freedom (3 for each unconstrained grid point) remained. The total number of degrees of freedom for fluid and structure thus led to mass and stiffness matrices for Equation (7) of order 659. Eigenvalue extraction of these large unsymmetrical matrices would have required a time-consuming complex extraction routine. It was decided, therefore, to attempt to reduce the

computer effort required without any significant sacrifice of accuracy.

In Equations (2) and (7), the  $Q$  matrices, which contain a factor of  $1/c$ , represent the effect of compressibility of the fluid. This effect is not considered significant except for high frequencies or in confined fluid spaces. Most analyses, including that of Everstine,<sup>1</sup> have incorporated the simplifying assumption of incompressibility; as a result,  $1/c$ , and hence  $Q$ , are zero. This assumption was not included in the formulation of Equation (7), which was set up for ready computer application, because there was little advantage in doing so.

When  $Q$  is taken to be zero, Equation (7) is readily reduced to

$$[M + \rho L H^{-1} L^T] \{ \ddot{u} \} + [K] \{ u \} = \{ F \} \quad (8)$$

One additional significant operation, that of obtaining the inverse of  $H$ , is required to set up Equation (8). However, this and the eigenvalue extraction operations are performed on matrices about one-half the size of those of Equation (7). Furthermore, the matrices of Equation (8) are symmetrical. The term  $\rho L H^{-1} L^T$  is interpreted as the added effective mass of the fluid. It is clear that fluid on only one side of the propeller blade may be idealized, and the added mass term can be made to represent fluid on both surfaces by using a value for fluid density,  $\rho$ , that is double the actual value.

No standard NASTRAN solution option, or "rigid format," is available to formulate and solve Equation (8). Executive modules can be manipulated, however, though the Direct Matrix Abstraction Program (DMAP) capability, and existing rigid formats may be altered in the same way. These capabilities were used to devise a procedure for implementing Equation (8).

First, the fluid matrix (or rather,  $(1/\rho)H$ ) was computed and made available for later reference. This fluid "stiffness" matrix was produced by making a static stress run on the fluid mass with material properties and boundary conditions as discussed above. ASET1 cards were used to specify that the solution set be retained only at the interface grid points, and an "OUTPUT1" DMAP ALTER instruction to specify that the resulting condensed stiffness matrix (or  $H$ ) be saved on a permanent file. Another ALTER instruction was used to stop further execution of the problem. This run can also be used to obtain terms of the  $L$  matrix. It was suggested previously that areas associated with each structural interface grid point can be used as  $L$  matrix terms. Calculating these areas and obtaining their projections in the three coordinate directions for a propeller surface can be quite difficult. It is much easier, and equivalent, to specify a unit pressure loading on the interface and request a printout of the three equivalent nodal forces on these grid points. The forces will thus be calculated in a consistent manner. These forces can be used to make up the  $L$  matrix. They are functions of only the pressurized surface shape and the location of the grid points. Therefore, since these two quantities are identical for both the structure and the fluid at their interface, the unit pressure load can be applied to the idealized fluid interface in the same run from which the  $H$  matrix is obtained. The equivalent nodal forces can then be entered on DMIG cards as  $L$  matrix terms. Since the fluid run has only one degree of freedom, while all three translational degrees are needed to obtain the three components for each surface grid point, the equivalent force matrix must be printed out before constraints are applied. This printout is requested through another ALTER instruction.

To summarize the procedure: a static stress run is started on the fluid mass with unit pressure applied to the interface. All interface grid points are specified on ASET1 cards. The stiffness matrix (after constraints and condensation are applied) is placed on a permanent file via the required control card. An OUTPUT1 ALTER instruction and the equivalent nodal forces are then printed out, at which point the calculation is stopped. The matrix condensation is not theoretically required, but is done to save space; it does not affect the final results.

Equation (8) may be set up for the propeller and solved to obtain either the frequency response or the dynamic response to applied time-dependent forces by running the propeller data with the additional data already obtained. The natural frequencies are obtained by specifying a modified natural modes calculation with  $F$  null (Rigid Format 3); the dynamic response is obtained by specifying a transient response calculation with  $F$  input (Rigid Format 9). Each of these rigid formats requires its own ALTER routine, although each routine works in essentially the same way, and the additional input is handled similarly. Structural grid point data must include one extra scalar point (SPOINT) for each fluid interface grid point listed on ASET1 cards and thus retained as a degree of freedom in the  $H$  matrix calculation. These scalar points are dummy grid points which have no coordinates, but have one allowable degree of freedom each (the zero component). They are established by listing their identification numbers on SPOINT cards. These identification numbers are (for convenience) the fluid interface grid point numbers, and they must be different from all propeller grid point numbers. The purpose of the scalar points is to expand the dimensions of the structural stiffness matrix, before

constraints are applied, sufficiently to accept the  $L$  (or  $L^T$ ) matrix which is also input to the stiffness matrix via DMITIG cards. It was found more advantageous to require the  $L^T$  matrix; the  $L$  matrix can readily be derived from it by transposition. The terms of the  $L^T$  matrix are specified on DMITIG cards, each of which relates one of the three nodal force components per unit pressure at a wetted propeller grid point, obtained from the fluid calculation with the zero component of the corresponding scalar point. If the algebraic signs of all of the  $L^T$  terms are reversed, those of  $L$  will also be reversed, and the added mass term,  $\rho L H^{-1} L^T$ , will be unchanged; therefore a sign error for the  $L^T$  matrix as a whole has no effect. Since only the interface fluid points are input here (as scalar points), the zero rows of  $L$  are eliminated so that the matrix conforms with the condensed version of  $H^{-1}$ . The  $(1/\rho)H$  matrix is obtained from the file on which it has been stored by including the required control card and an INPUT1 ALTER instruction.

Two partitioning matrices, named PVEC1 and PVEDC1, must also be input via DMI cards. These are column matrices having the dimensions  $(N+S) \times 1$ .  $N$  is the total number of structural degrees of freedom (number of grid points  $\times 6$ ) and  $S$  is the number of scalar points. For PVEC1, the first  $N$  terms are zero, and the remaining  $S$  terms are 1.0. PVEC1 is used to partition the stiffness matrix to obtain  $L^T$ , used with  $(1/\rho)H$  by the ALTER routine to form the added mass term  $\rho L H^{-1} L^T$ , which is then added to the structural mass matrix. Note that the inverse of  $(1/\rho)H$  is  $\rho H^{-1}$ . For the PVEDC1 matrix, all  $(N+S)$  terms are zero. PVEDC1 is used to form a "dummy" partition on the "augmented" mass matrix, which now includes the added mass terms, so that the program will correctly perceive this matrix as symmetrical.

One final type of additional input is required: all scalar points must be listed on single point constraint (SPC) cards. These constraints are in addition to whatever constraints are applied to the propeller. It is suggested that 20-node three-dimensional CIHEX2 elements, with two integration points specified, be used to represent both the fluid and the propeller, and that the consistent mass matrix formulation be specified for the propeller.

The procedure just described can be used to obtain vibration modes and dynamic response of propellers under a variety of conditions of submergence. Partial submergence at any given instant can be represented during a fluid run by listing on ASET1 cards only the fluid grid points which correspond to submerged points on the propeller. During a structural run these points are listed on SPOINT cards. Also, the dimensions of the PVECI and PVECDI column matrices must be adjusted by making the number of terms with value of 1.0 at the end of the PVECI column equal to the number of wetted grid points. Wetting of both surfaces of the blade is simulated by using double the actual value of fluid density,  $\rho$ , for the fluid run. Wetting of only one surface, such as occurs during supercavitation, is represented by use of the actual value of  $\rho$ .

This procedure can be extended, without further DMAP program modifications, to analyze dynamic response of partially submerged propellers and to take into account the progressively changing degree of submergence. The extended procedure consists essentially of running the analysis in separate steps, one for each arbitrarily chosen stage of submergence. A convenient way to determine a new stage of submergence is to consider the wetting of a new row of propeller elements. This extended procedure was

devised and was applied to an existing propeller for which some experimental and analytical data were available. The details of this application will be presented later. The finite element idealization of this blade was laid out so that one series of element boundaries coincided with water lines on the propeller blades as it progressed into the water during each revolution. There were two such boundaries in this rather coarse idealization, defining three rows of elements; hence, three stages of submergence were assumed.

The fluid run, to obtain the condensed  $(1/\rho)H$  matrix, was run once for each stage of submergence. For each run, the solution set of wetted grid points, as defined by ASET1 cards, contained only the points presently wetted, i.e., points just submerged plus all points previously submerged. Similarly, unit pressure was applied to the corresponding wetted element faces to obtain the  $L^T$  matrix terms for the same wetted points. Finally, those interface grid points not yet submerged had to be considered part of the fluid boundary and were constrained. Constraints were, of course, removed from those points as they became submerged in subsequent stages and added to those included on ASET1 cards. Each of the  $(1/\rho)H$  matrices thus produced and stored on a permanent file was assigned a separate name; in this case the names used were HMATRIXSTEP1, HMATRIXSTEP2, and HMATRIXSTEP3. Such separate identification of the  $L^T$  matrices was not necessary, as they are manually punched on DMIG cards and input separately to the structural computer runs. The structural run in this case was also carried out once for each stage of submergence, but all except the first were restart runs. Thus, all but the last run was checkpointed.

The series of runs is set up as follows. First, time-dependent forces are specified for the selected grid points by means of the required DAREA, DLOAD, TABLED1, and TLOAD1 cards. The time spanned by these forces covers the entire time for which the analysis is applied. The time at which the force is initiated at each selected grid point is dictated by the speed of rotation of the propeller and by the location of the point. The user must also specify the length of each integration time step, and the number of steps, on a TSTEP card. The calculation is terminated when the time defined by the product of time step x number of steps on the TSTEP card has elapsed. If a uniform time step is used throughout, the number of steps may be specified to make each run cover just the length of time required for the water line to progress from the first to the second boundary defining the present stage of submergence. The first run and each restart then require a different TSTEP card (unless, by coincidence, each stage of submergence lasts the same length of time). Other changes must also be made between runs. Scalar points for all interface fluid grid points which are to be wetted at any time during the analysis must be input (on SPOINT cards) for the first run, and this does not change for succeeding restarts. The same is true of the scalar point constraints. The PVECD1 matrix is also input as before, with column dimension equal to six times the number of propeller grid points plus the number of scalar points, and it is not changed. The PVEC1 column matrix is now replaced by a series of matrices, one for each structural run, and they may be designated PVEC1, PVEC2, and PVEC3. The column dimension is the same for all of these, and is the same as that of PVECD1. The number and location of the "1.0" terms, however, must correspond to the total set of wetted

devised and was applied to an existing propeller for which some experimental and analytical data were available. The details of this application will be presented later. The finite element idealization of this blade was laid out so that one series of element boundaries coincided with water lines on the propeller blades as it progressed into the water during each revolution. There were two such boundaries in this rather coarse idealization, defining three rows of elements; hence, three stages of submergence were assumed.

The fluid run, to obtain the condensed  $(1/\rho)H$  matrix, was run once for each stage of submergence. For each run, the solution set of wetted grid points, as defined by ASET1 cards, contained only the points presently wetted, i.e., points just submerged plus all points previously submerged. Similarly, unit pressure was applied to the corresponding wetted element faces to obtain the  $L^T$  matrix terms for the same wetted points. Finally, those interface grid points not yet submerged had to be considered part of the fluid boundary and were constrained. Constraints were, of course, removed from those points as they became submerged in subsequent stages and added to those included on ASET1 cards. Each of the  $(1/\rho)H$  matrices thus produced and stored on a permanent file was assigned a separate name; in this case the names used were HMATRIXSTEP1, HMATRIXSTEP2, and HMATRIXSTEP3. Such separate identification of the  $L^T$  matrices was not necessary, as they are manually punched on DMIG cards and input separately to the structural computer runs. The structural run in this case was also carried out once for each stage of submergence, but all except the first were restart runs. Thus, all but the last run was checkpointed.

The series of runs is set up as follows. First, time-dependent forces are specified for the selected grid points by means of the required DAREA, DLOAD, TABLED1, and TLOAD1 cards. The time spanned by these forces covers the entire time for which the analysis is applied. The time at which the force is initiated at each selected grid point is dictated by the speed of rotation of the propeller and by the location of the point. The user must also specify the length of each integration time step, and the number of steps, on a TSTEP card. The calculation is terminated when the time defined by the product of time step x number of steps on the TSTEP card has elapsed. If a uniform time step is used throughout, the number of steps may be specified to make each run cover just the length of time required for the water line to progress from the first to the second boundary defining the present stage of submergence. The first run and each restart then require a different TSTEP card (unless, by coincidence, each stage of submergence lasts the same length of time). Other changes must also be made between runs. Scalar points for all interface fluid grid points which are to be wetted at any time during the analysis must be input (on SPOINT cards) for the first run, and this does not change for succeeding restarts. The same is true of the scalar point constraints. The PVECD1 matrix is also input as before, with column dimension equal to six times the number of propeller grid points plus the number of scalar points, and it is not changed. The PVEC1 column matrix is now replaced by a series of matrices, one for each structural run, and they may be designated PVEC1, PVEC2, and PVEC3. The column dimension is the same for all of these, and is the same as that of PVECD1. The number and location of the "1.0" terms, however, must correspond to the total set of wetted

interface points as represented by the scalar points during each run. The DMAP ALTER instruction which utilized PVEC must also be changed from run to run to call for the currently available PVECl matrix. Another ALTER instruction, as well as a control card, must be changed for each run to obtain the required  $(1/\rho)H$  matrix for each stage. Finally, each run must also have a new  $L^T$  matrix input via DMIG cards. Since this information is part of the bulk data, the previous  $L^T$  matrix must be eliminated during each restart.

Sample input for a vibration problem and for a transient response problem are presented in the appendix.

#### VIBRATION ANALYSIS OF P3604 PROPELLER

The vibration analysis procedure was first applied to a supercavitating propeller, P3604, for which finite element idealization data were already available from a previous stress study. The blade was divided into 16 isoparametric, 20-noded, three-dimensional elements, with 155 grid points (Figure 1). A quantity of water three elements thick, extending one element beyond the edges of the blade, and generally following the twist of the blade, was assumed. The elements were roughly cubical, and the thickness of the water modeled was about one-half to two-thirds the length of the blade. This size was judged to be sufficient to represent an infinite body of water, based on a study of the results presented by Marcus.<sup>4</sup> With the procedure used here, larger representations could be investigated at fairly moderate cost. The double value of water density was input to represent water on both sides of the blade. This fluid idealization consisted of 578 grid points and 90 elements. A total of 263 degrees of freedom remained after constraints were applied. The fluid-structure

interface surface contained 65 grid points, which were retained in the  $H$  matrix. The  $L^T$  matrix terms numbered  $65 \times 3$  or 195. However, nine of the interface points were adjacent to the base grid points of the propeller, which were later to be constrained. The corresponding  $9 \times 3$ , or 27  $L^T$  matrix terms were therefore not included on DMIG cards. Space was later reserved for them in the propeller matrices, however, as 65 scalar points were input, but the  $L^T$  boundary terms which were not input were implicitly zero. It was not necessary to leave out these terms; they would be eliminated later by constraints. With this procedure, the pressures in the water at the nine base grid points were not constrained to zero, even though deflections of the corresponding propeller grid points were constrained. The five lowest natural frequencies of the blade in water were calculated and are presented, with the corresponding calculated in-air frequencies, in Table 1. The modal deflection data indicated that the first mode of vibration consisted of nearly pure spanwise bending, while the other modes contained a combination of torsion and chordwise bending. Although no experimental data exist to compare with this sample calculation, the results appear to be consistent with experimental results for more conventional blades, particularly for the first mode. It seems rather remarkable that the ratios of frequencies in water to those in air are fairly constant, ranging from 0.46 to 0.55, for all modes. This was not expected because of the large differences in thickness of the blade and the variety of possible vibration modes. This phenomenon may not be characteristic of other blade geometries.

The version of NASTRAN used for these analyses was Level 17. Procedures for both the vibration and transient analyses are listed in the Appendix.

#### TRANSIENT RESPONSE ANALYSIS OF SES-100B PROPELLER

After this work was underway, some full scale test results, including both vibration and transient response data, became available<sup>5,6</sup> for the SES-100B controllable pitch, partially submerged, supercavitating propeller (number 7016.3). Allison's work<sup>5</sup> also contains finite element analyses of the vibration modes and transient response of this blade, utilizing 276 grid points and 279 plate bending elements. Calculated transient forces were used, and a constant physical mass of water of approximately conical shape circumscribing the blade, was taken as added effective mass. One-half of the imaginary cone of water was actually used to simulate full cavitation. Transient response, in the form of measured stresses at a gage near the root of the blade, was plotted versus time for the period during which the blade enters the water and reaches maximum submergence.

The SES-100B propeller was selected for this transient response analysis because of the availability of geometrical and test data. Due to the developmental nature of this application, however, and to time and cost constraints, the idealization constructed was rather coarse, consisting of 96 grid points and nine CIHEX2 isoparametric three-dimensional elements. A detailed study of this blade would require a finer idealization, particularly so because it contained an annex, or discontinuity, in the pressure surface curvature. The exercise of engineering judgment attempted to compensate for this coarseness in constructing the idealization, in which, for instance, thicknesses at grid points do not all coincide exactly with those on the actual blade. One of the constraints on placement of element boundaries was to require that one set of boundaries coincide with water

lines at successive assumed stages of submergence of the blade. This constraint would not be necessary with a fine idealization.

A view of the blade, looking in the forward direction, is shown in Figure 1. A series of water lines at various stages of submergence was constructed from data reported by Lewis<sup>6</sup> and drawn on Figure 1. An idealization was constructed with two of the element boundaries approximately coinciding with two water lines, and this is shown in Figures 2 and 3. In these figures the water lines are shown slightly curved because the view of the propeller is flattened. The location of the strain gage from which Allison's transient response data<sup>5</sup> were obtained is also shown in Figure 2. For the first arbitrarily-defined stage of submergence, elements 7 through 9 are submerged; for the second stage, elements 4 through 9 are submerged; and for the third stage, all elements are submerged. The fluid mass idealized for this case was of approximately the same size and shape relative to the blade as for the P3604 vibration analysis, but the fluid for the SES-100B was divided into only two layers. An outline of one face of the fluid mass, showing the fluid-structure interface, is shown in Figure 4. The entire fluid mass is shown in Figure 5.

The operating conditions for which this calculation was carried out were the design conditions of 85 knots, 1870 rpm, and 33-degree blade pitch. Blade pressures are discussed by Allison<sup>5</sup> and Lewis,<sup>6</sup> both of whom considered the pressure at each point to be applied in three stages. First was an impact pressure, computed according to a theory by Pierson,<sup>7</sup> followed by an entry pressure predicted from a theory by Wang.<sup>8</sup> Finally, a steady value was reached, the value predicted from a theory by Yim. The same procedure was followed here to calculate forces to apply to grid

points 73, 75, 47, 49, 21, and 23. These are mid-side nodes and are so situated that force is applied to each when the propeller reaches the mid-point of its stage of submergence. The pressure versus time plot at each of these grid points was derived from data given by Lewis.<sup>6</sup> These plots are presented in Figure 6 and show that these are essentially pulse pressures with no oscillating component.

The transient response analysis consisted of one fluid and one propeller computer run for each stage of submergence, a total of six runs. Stresses are printed out in NASTRAN at the grid points and at the element centroids. Unfortunately, it was not feasible to place a grid point exactly where experimental data were available. Therefore, stresses computed at three grid points (22, 36, and 39) which surround this point (shown as Gage 1 in Figure 2) were plotted and the plots are shown in Figures 7, 8, and 9. Static stresses were also calculated and plotted on these same figures. The three portions of the dynamic forces were averaged and applied at the same points to obtain these static stresses. The dynamic pressures were also applied, but with the steady state value truncated, to the propeller in air, and the results are given in Figures 10, 11, and 12. The plot of dynamic stresses, reproduced from Allison's paper,<sup>5</sup> is presented here as Figure 13. Natural vibration frequencies for the SES-100B propeller at the three stages of submergence were also calculated and are presented in Table 2.

#### DISCUSSION OF SES-100B ANALYSIS RESULTS

The primary purpose of this analysis was to verify the computational procedures developed and to produce results that appear reasonable and that provide some insight into the behavior of such propellers. It was also

desired that, despite the coarseness of the idealization, some meaningful comparisons could be made with experimental data.

The plots of transient stresses in the propeller in water (Figures 7, 8, and 9) show that the peak stresses at the three locations plotted range from 21500 to 32000 psi. The measured peak stress shown in Figure 13 is about 31000 psi. This apparent close agreement is probably fortuitous. The stress amplitudes shown in the analytical plots vary with a predominant frequency equal to the lowest natural frequency of the propeller, as verified by the natural frequency analysis. What appears to be a similar predominant vibrational component, with nearly the same frequency, is displayed in the experimental plot (Figure 13). Substantial amplitude damping is evident in the experimental plot, however, even within each complete period of vibration.\* Both the analytical and experimental plots indicate that the blade vibrates through several complete cycles before becoming fully submerged. Thus, pressure due to submergence in the later stages are applied when the existing calculated amplitudes of deflection are in error, due to the lack of damping. Furthermore, the calculated phase could be in error due to the probable slight inaccuracy of the calculated natural frequencies. Calculated response due to these later water entry pressures may therefore detract from, rather than improve, accuracy of the overall dynamic response. The calculated stress-time plots show no apparent reaction to these later stage pressures, however. This is evidently because the last part of the propeller to enter the water is the portion close to the hub where lower pressures are generated at impact (due to the smaller

---

\*Damping was not accounted for in the analysis, but could be, as discussed later.

radii and hence lower linear velocity resulting from rotation) and impact pressures produce smaller bending moments due to the smaller effective moment arms. The plot of calculated stress versus time is probably meaningful quantitatively only to the first peak if damping is not accounted for. Fortunately, this portion of the curve, or more particularly the value of this peak, is of primary interest.

Two other features of these curves are significant. First, peak stress values are practically the same for the in-water and the in-air cases. Second, these peak values are on the order of two to three times the static values. This suggests that, for this approximately pulse-type pressure application, the blade behaves somewhat like a weight suddenly suspended by a spring: the weight oscillates about the static equilibrium point with an amplitude double the static deflection. However, the ratios of the dynamic to static stresses in the propeller blade probably vary at different locations because of the complicated shape. For this particular example, a Fourier series representation of the assumed pressure pulses apparently would not contain any strong components near any of the natural frequencies in water or in air. The damping effect of water no doubt serves to decrease peak dynamic stresses slightly, but the main effect of submersion in water, apart from transmitting force to the blade, appears to be in altering its natural frequencies. If a detailed study of a propeller were to be made, it would probably be wise to obtain stresses at all grid points (at least all the points on one surface) because a resonance magnification might occur locally, and hardly show up at the root of the blade.

The fundamental, or lowest, natural frequencies of the blade in air and in water may be derived from the stress versus time plots since the time record is probably long enough. All three plots for the in-air case display frequencies of about 650 Hz, slightly higher than the calculated natural frequency of 624 Hz shown in Table 2. The plots indicate that in water the blade rings at a fairly constant frequency of about 510 Hz, which is close to the natural frequency of 524 Hz calculated for the blade under its first stage of submergence. During most of the time covered by the plots, however, the blade is fully submerged, and one would expect the frequency to fall to about 420 Hz. A smaller initial stage of submersion, for which the fundamental frequency is higher, might produce a correspondingly higher ringing frequency. In this case, however, the initial load would also be smaller, being applied to the smaller area of the blade, and might not predominate as it does in the present case.

Damping (either hydrodynamic or structural) could readily be accounted for in this analysis, but the values of damping terms would have to be determined by the user, probably empirically. All damping would be accounted for in the structural computations. Since damping terms can be derived from the relative amplitudes of successive cycles of a freely vibrating structure, plots such as Figure 13, in which the attenuation of amplitude after initial response is clearly illustrated, could probably be used for this purpose. The principal effect of damping on peak calculated stresses would probably occur when two or more substantial dynamic forces are applied, separated by time intervals of the order of one-half a fundamental period.

It would be pointless to carry the analysis further in time to cover the emergence of the blade from the water, since the dynamic forces applied at that time would result essentially from releasing the relatively small steady state submergence pressures. These forces would be much less severe than those at entry.

It has been assumed in this analysis that dynamic behavior of a propeller can be adequately described by analysis of a single blade, fixed along its base. Errors due to this assumption may be significant in some cases, particularly for propellers without relatively massive hubs. The errors could be introduced in two ways. First, flexibility of the hub violates the assumption of complete fixity, leading to lower natural frequencies than calculated. This effect was noted by Allison<sup>5</sup> in connection with the SES-100B propeller and with tests of a single blade mounted in a test jig. Second, hub flexibility and lack of great mass may permit a significant degree of dynamic interaction among the blades. It is also possible that in some cases significant interaction may occur through the water between the blades.

The computational procedures followed here could no doubt be simplified and automated to some extent with the aid of further executive module programming.

#### CONCLUSIONS

1. Rational procedures have been presented for calculating the natural vibration modes and transient response of partially or fully submerged, supercavitating or conventional marine propellers. Cost of these analyses should be moderate, and they require only use of a standard NASTRAN program.
2. Both the vibration modes and the transient response analyses, particularly when progressive submergence is treated, need more verification.

3. For the essentially pulse-shaped pressure-time profile, as used here in the SES-100B propeller example, peak root stresses were predicted equally well whether the blade was considered in air or in water. This may not have been true of stresses elsewhere on the blade. Also, it may have been by chance that no resonances of the blade were excited by components of the assumed pressures. If time-dependent pressures with oscillatory components were applied, it is expected that peak stresses would be affected by submergence in water.

4. Calculated stresses indicated, as did published experimental results, that blade root stresses due to pulse pressures can be two or more times as high as calculated stresses based on the same pressures applied statically.

5. Detailed studies of stresses and deflections throughout typical propeller blades, utilizing finer finite element meshes would be useful in providing more information about response of typical propellers under various conditions.

6. When damping was not taken into account, transient response after about the first half of a fundamental vibration period was quite unrealistic, but peak stress values were apparently not affected. Damping constants need to be established, perhaps through an empirical approach. The apparent failure of the blade ringing frequency to fall promptly to the fully submerged value needs further investigation.

7. It would be worthwhile to simplify and automate, whenever possible, the procedures used here.

#### ACKNOWLEDGMENTS

The authors wish to express their gratitude to Mr. Myles Hurwitz for his help and advice regarding computational aspects of this project.

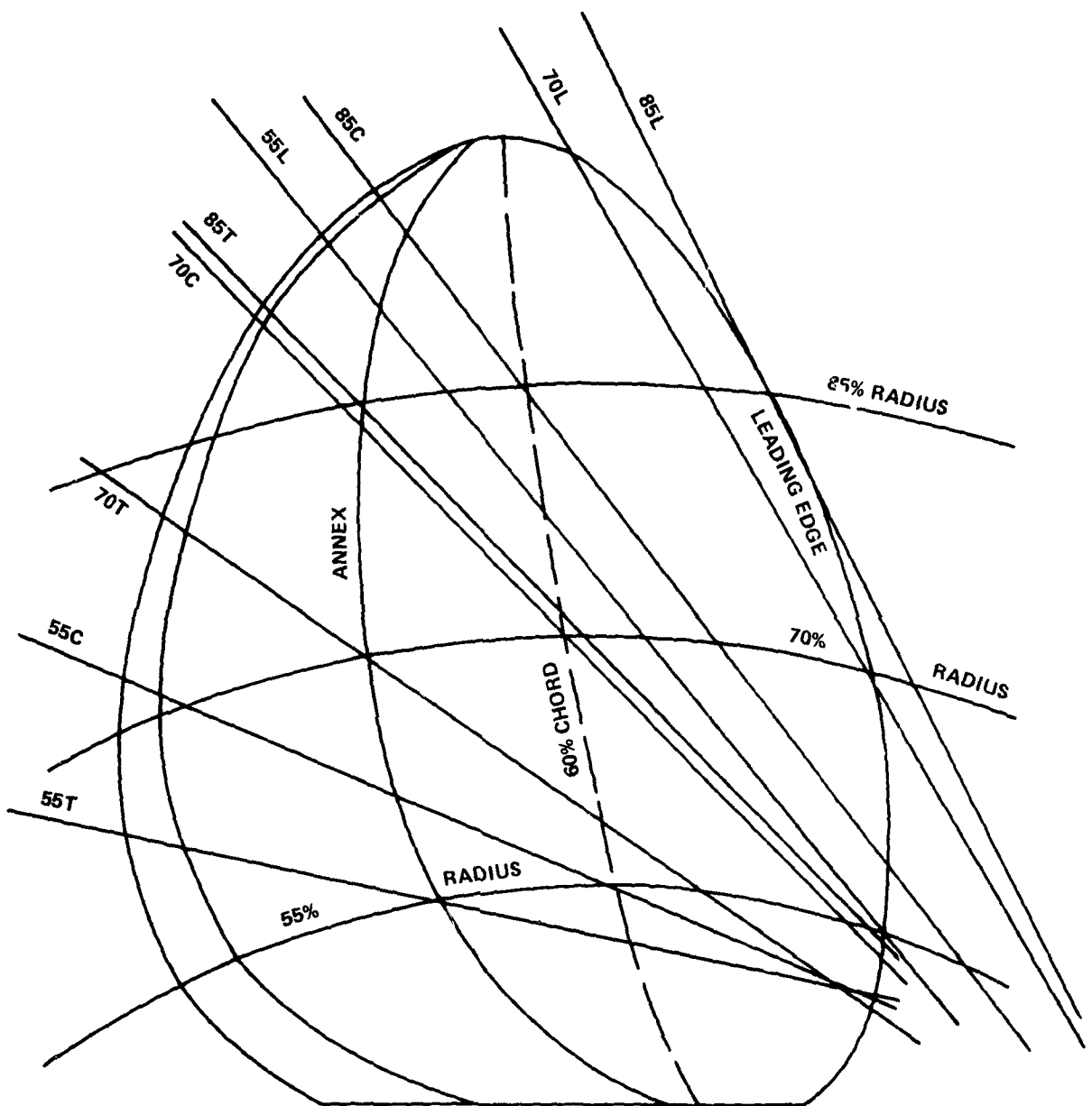


Figure 1 - SES-100B Propeller Blade with Waterlines

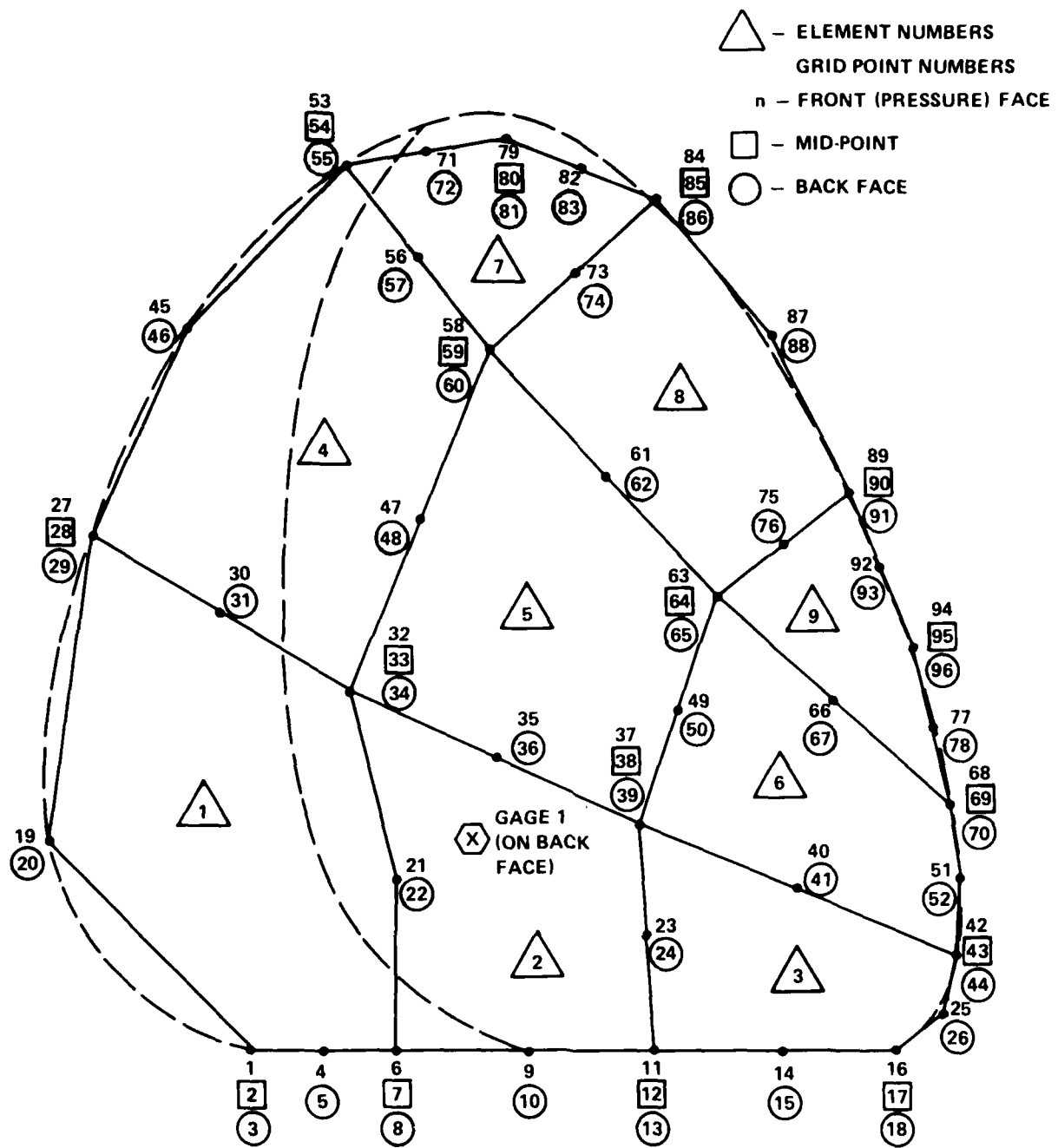


Figure 2 - Representation of Propeller Blade with Finite Elements

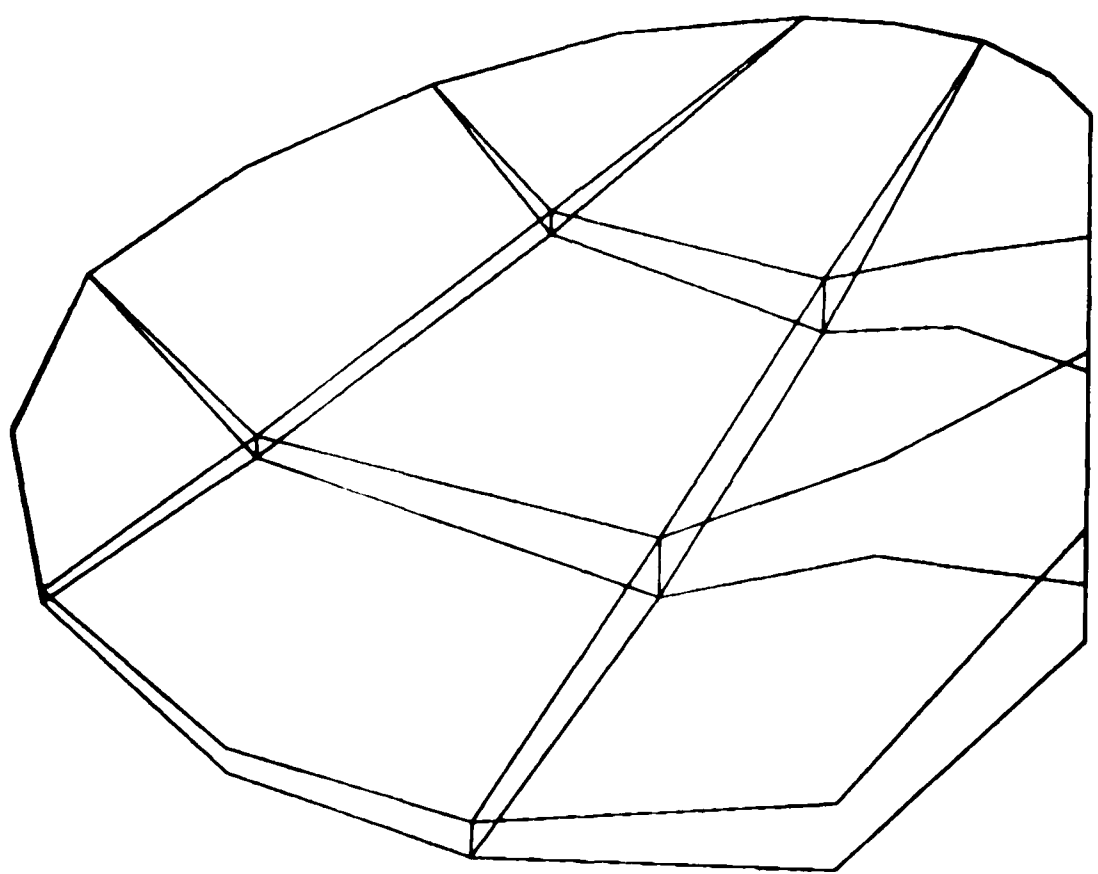


Figure 3 - Finite Element Idealization of Propeller Blade

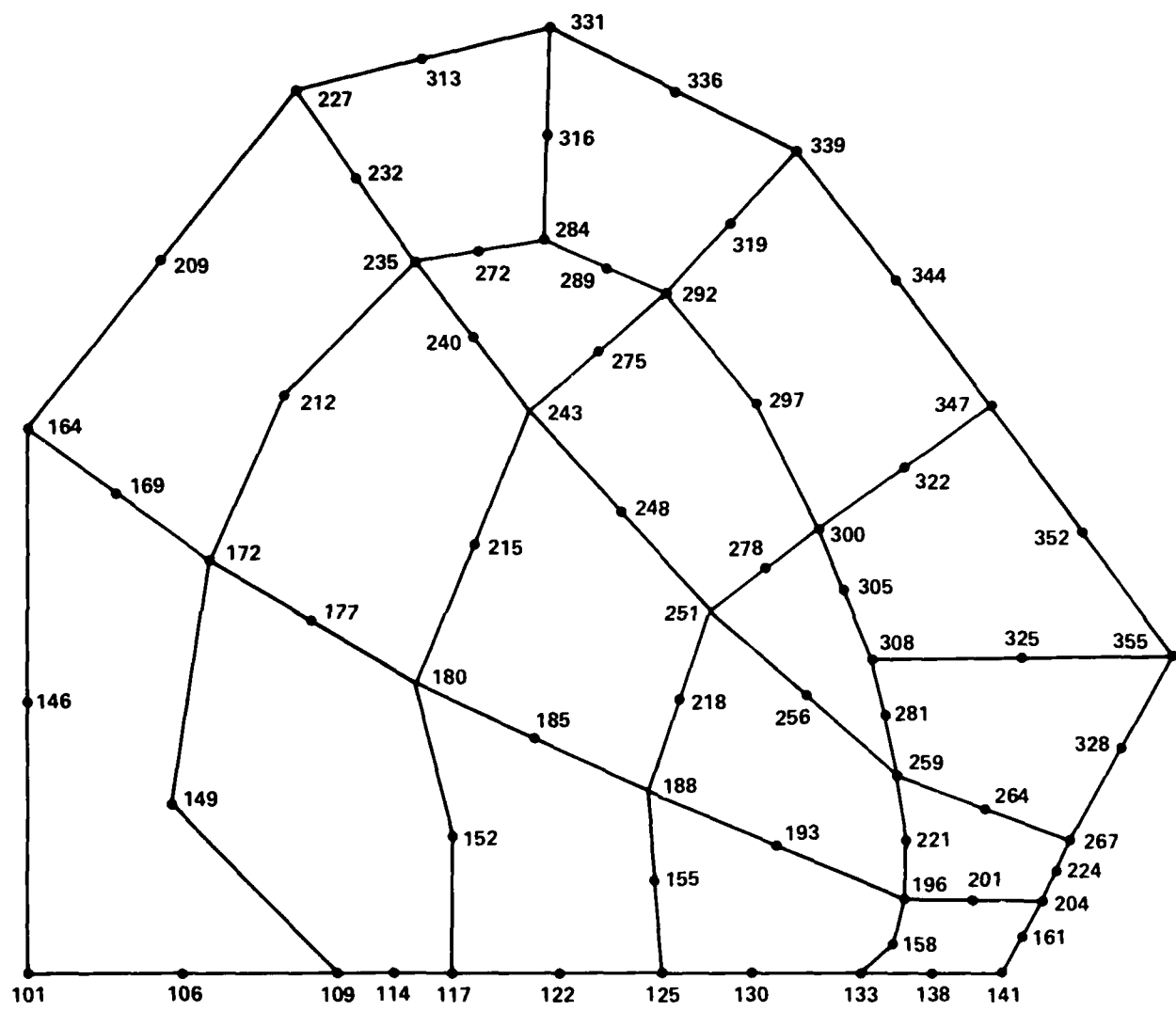


Figure 4 - Representation of Fluid-Structure Contact Face of Water Mass with Finite Elements

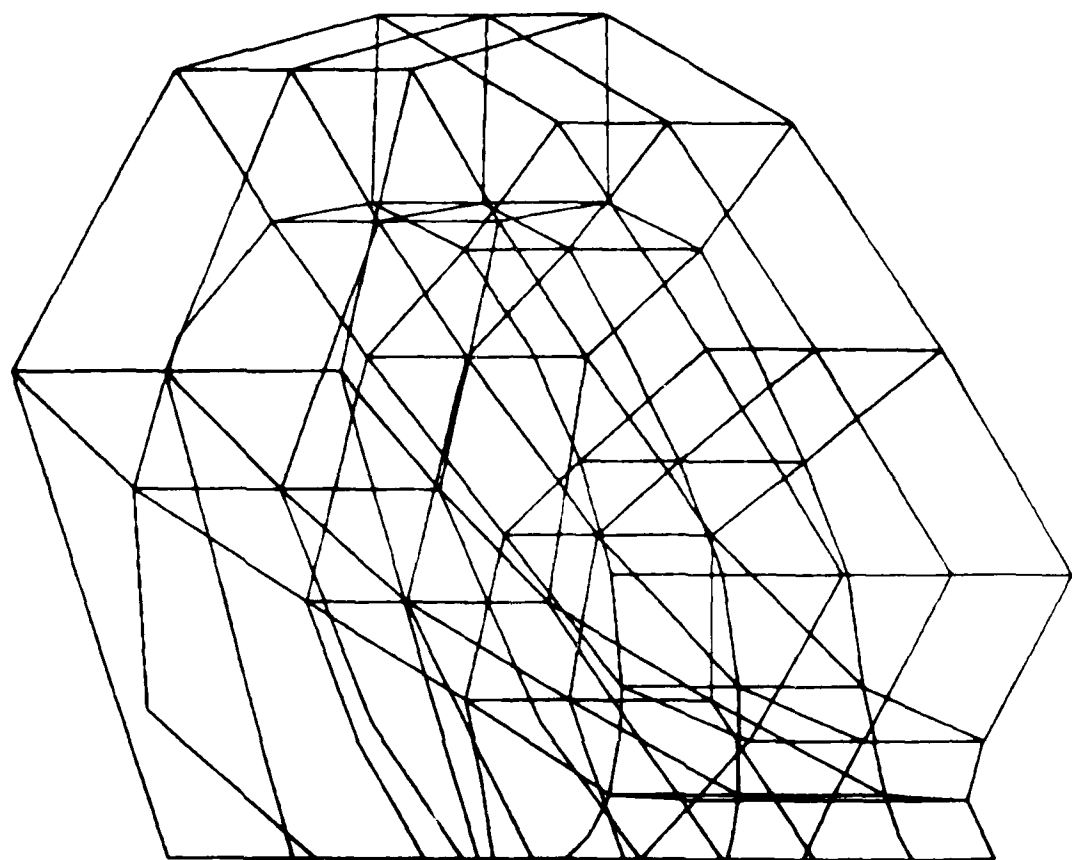


Figure 5 - Finite Element Idealization of Water Mass

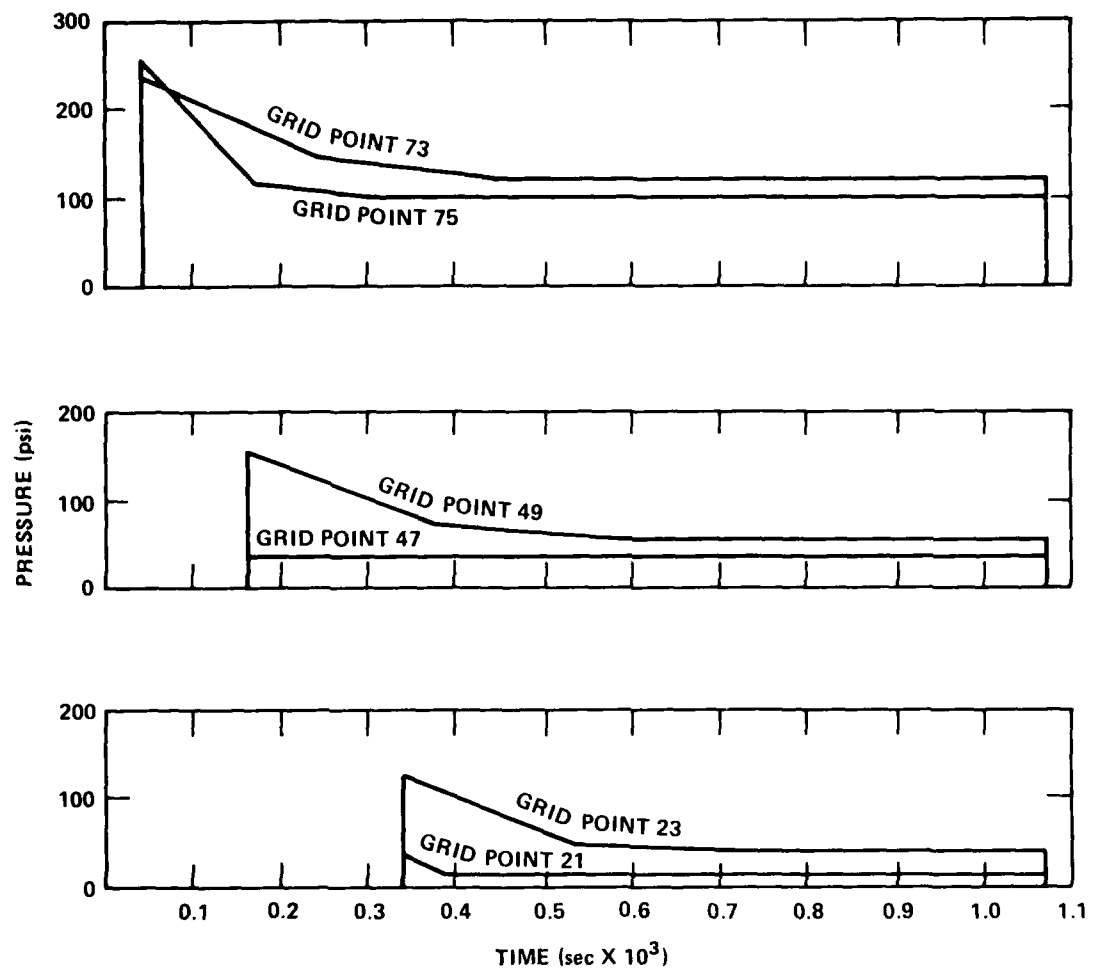


Figure 6 - Time-Dependent Blade Pressures

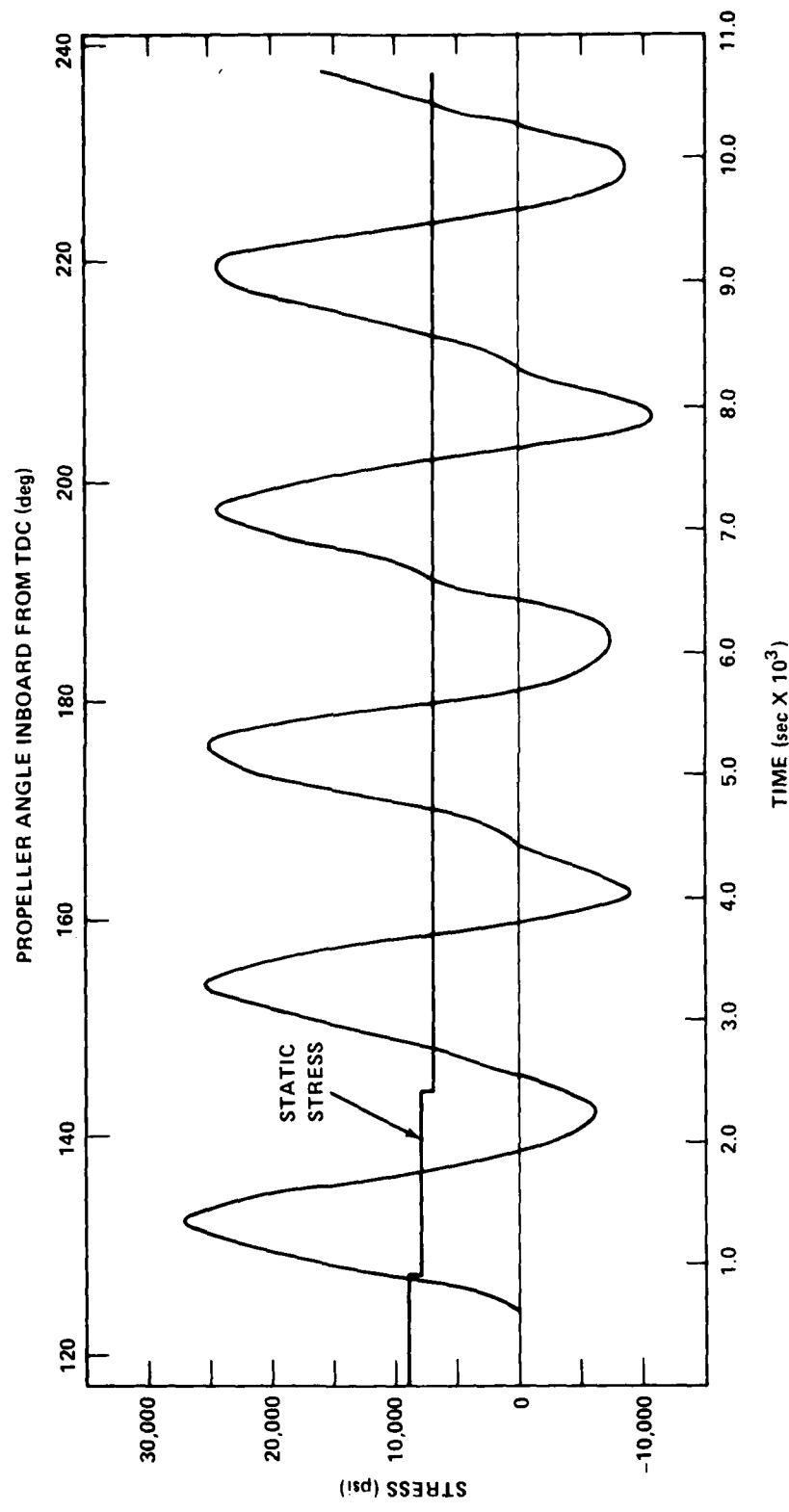


Figure 7 - Calculated Radial Stress in Progressively Submerging Propeller Blade  
at Grid Point 22

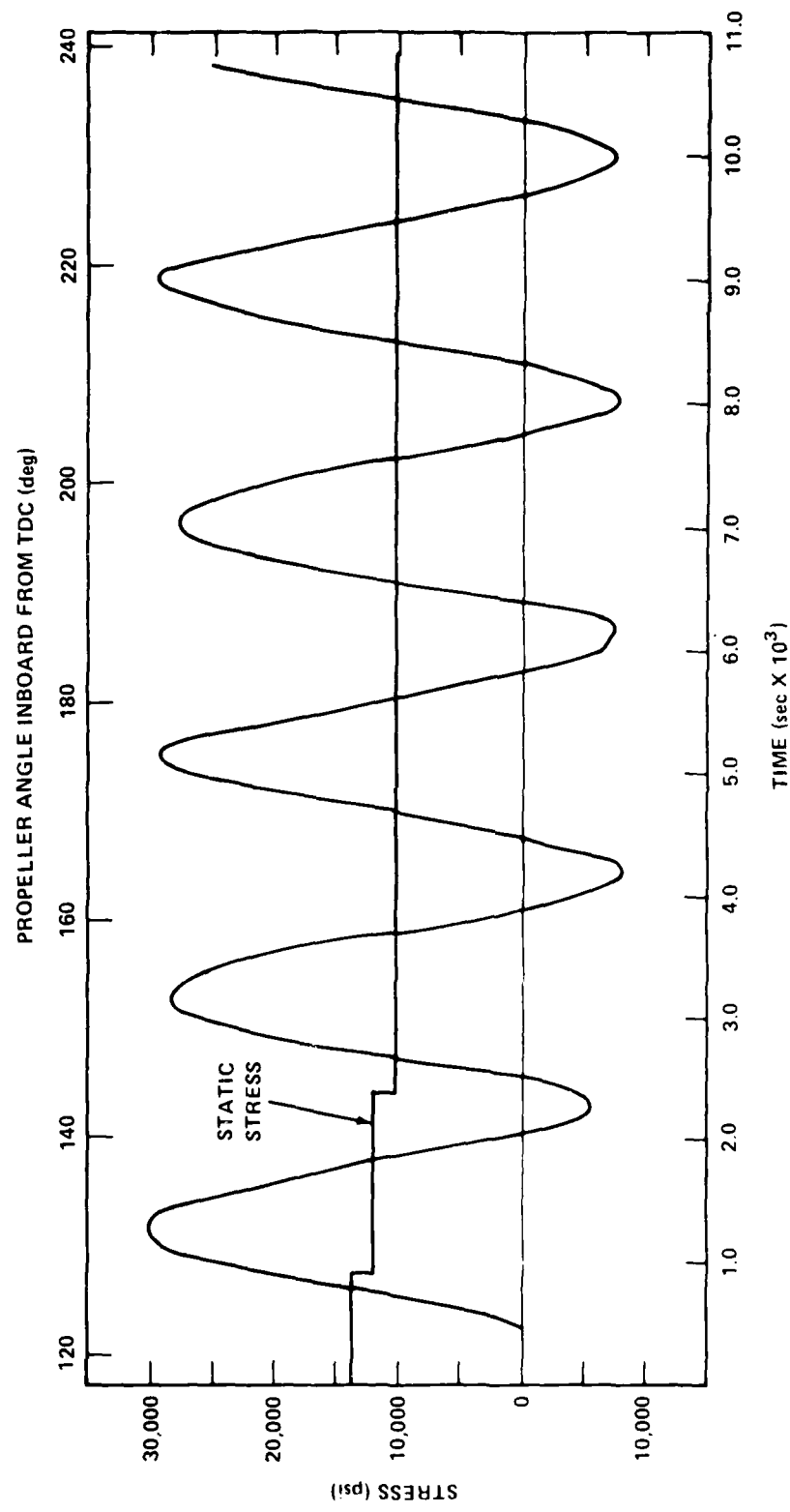


Figure 8 - Calculated Radial Stress in progressively Submerging Propeller Blade  
at Grid point 36

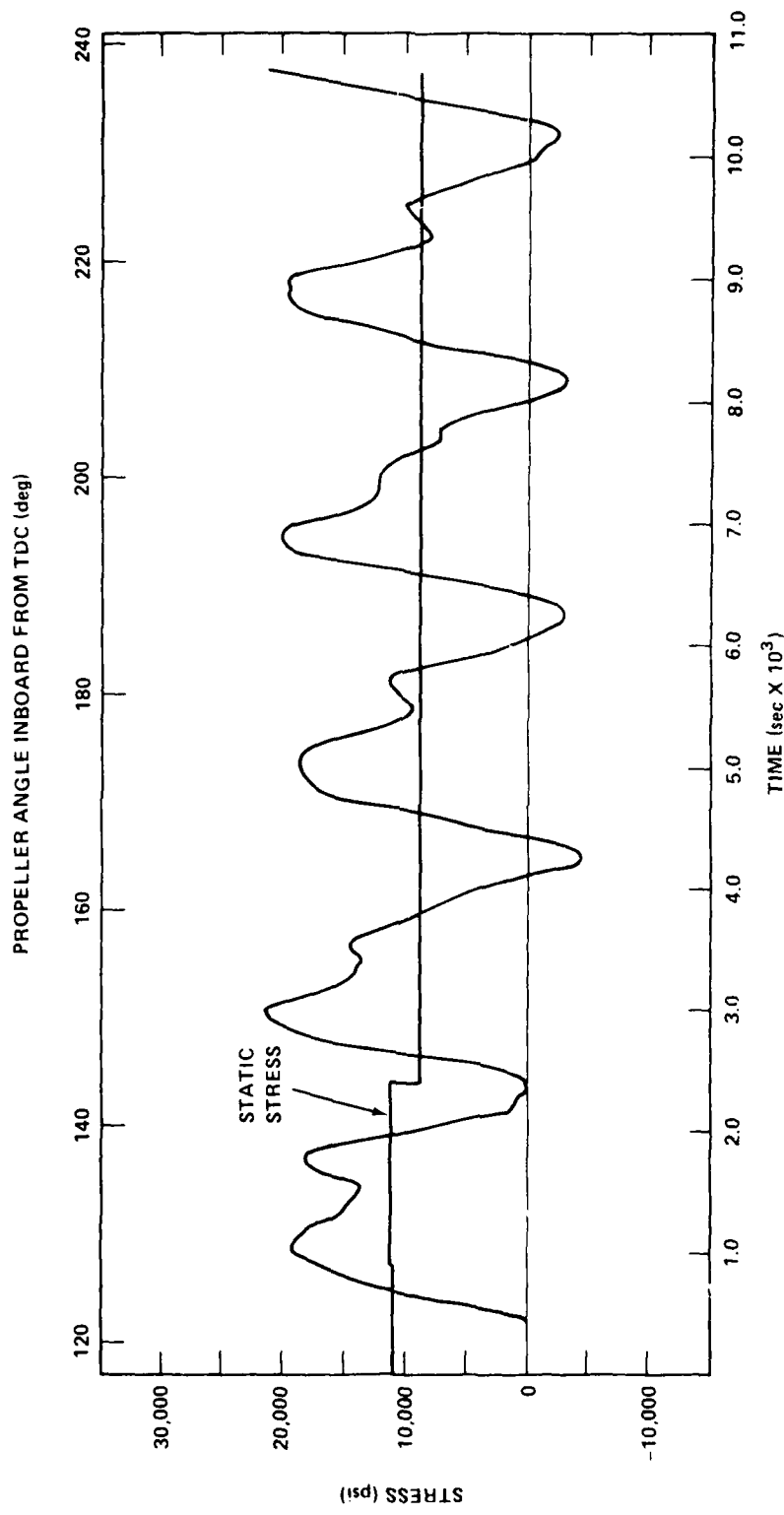


Figure 9 - Calculated Radial Stress in Progressively Submerging Propeller Blade at Grid Point 39

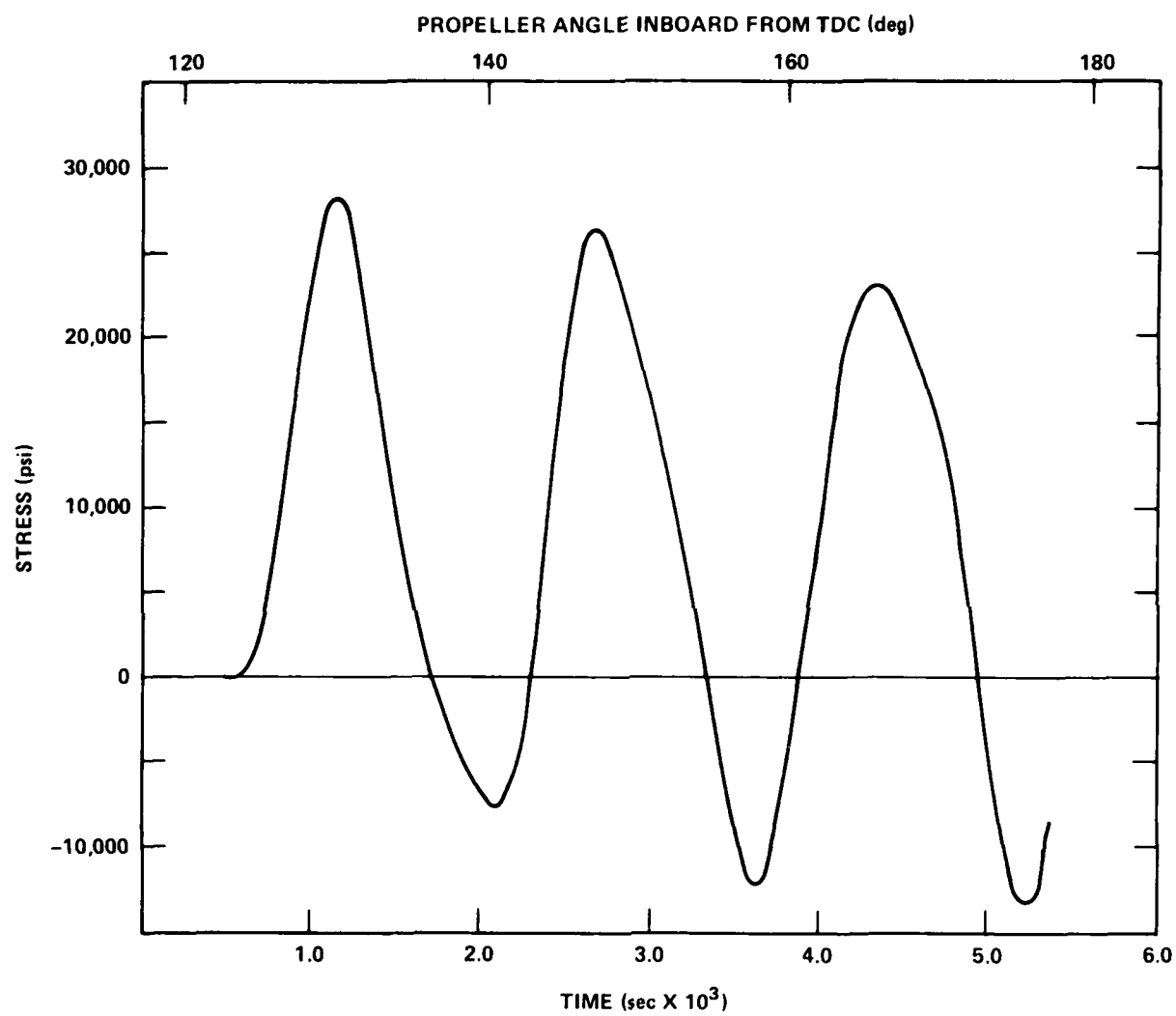


Figure 10 - Calculated Radial Stress at Grid Point 22 of Propeller Blade in Air with Applied Dynamic Forces

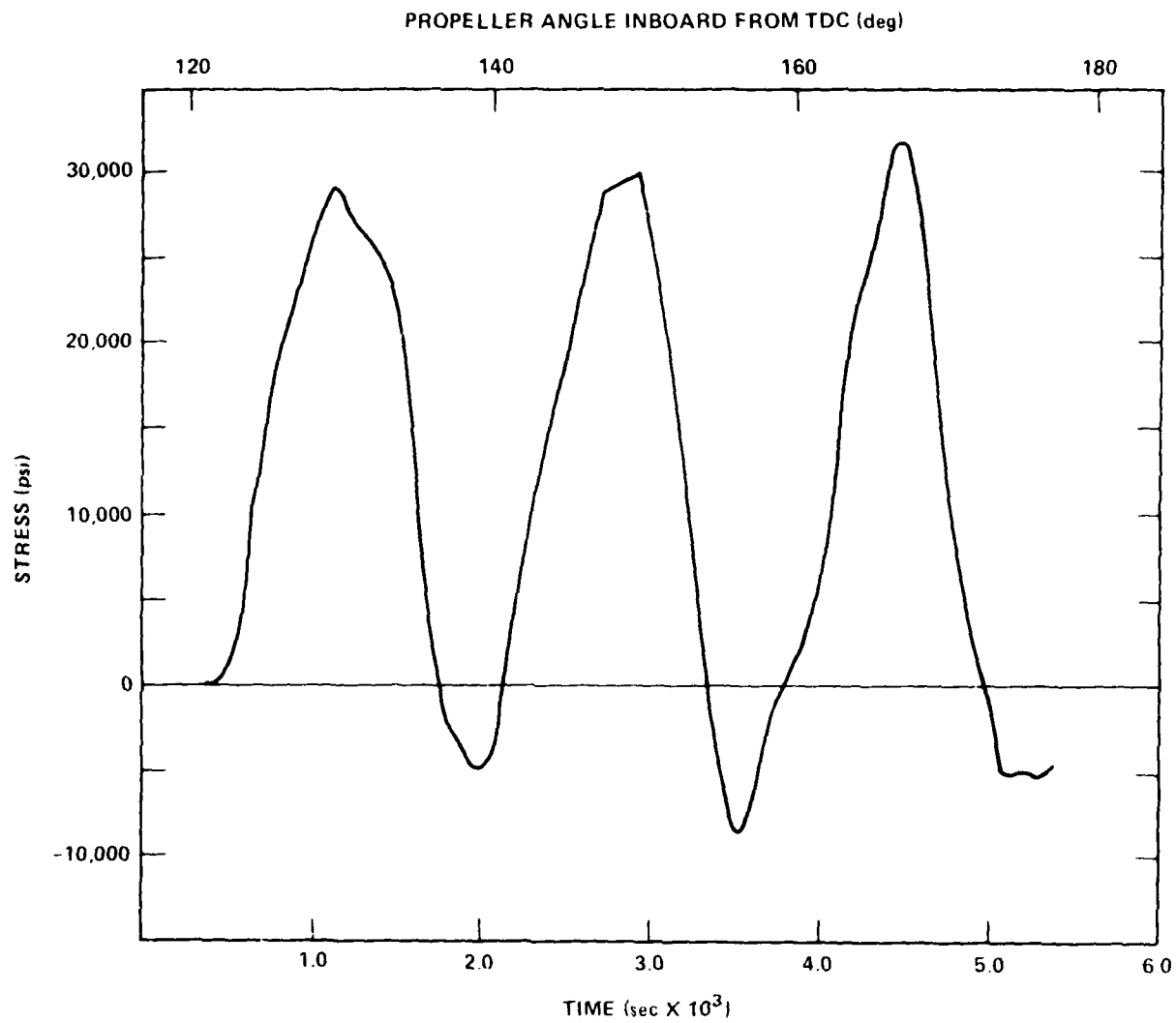


Figure 11 - Calculated Radial Stress at Grid Point 36 of Propeller Blade in Air with Applied Dynamic Forces

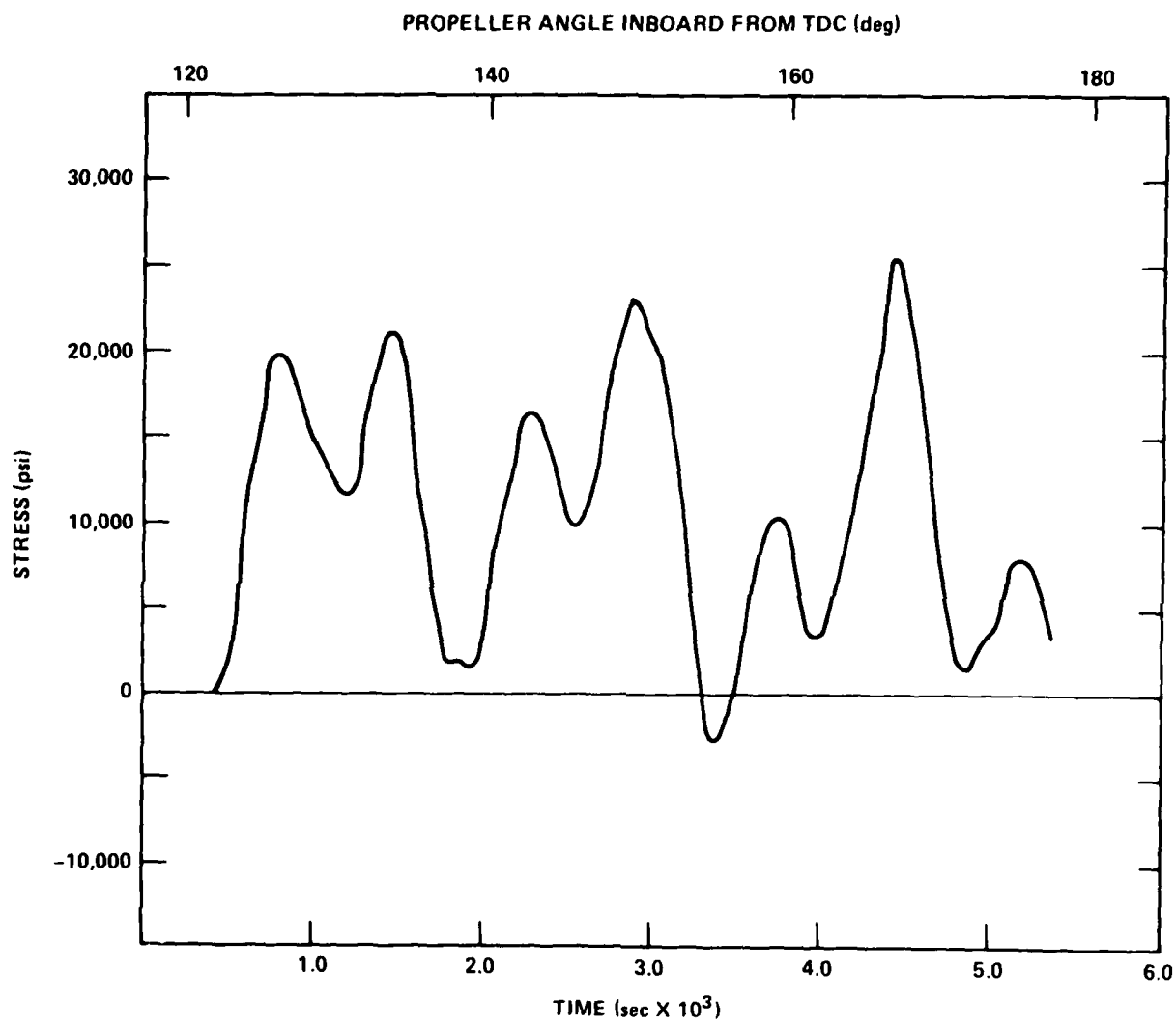


Figure 12 - Calculated Radial Stress at Grid Point 39 of Propeller Blade in Air with Applied Dynamic Forces

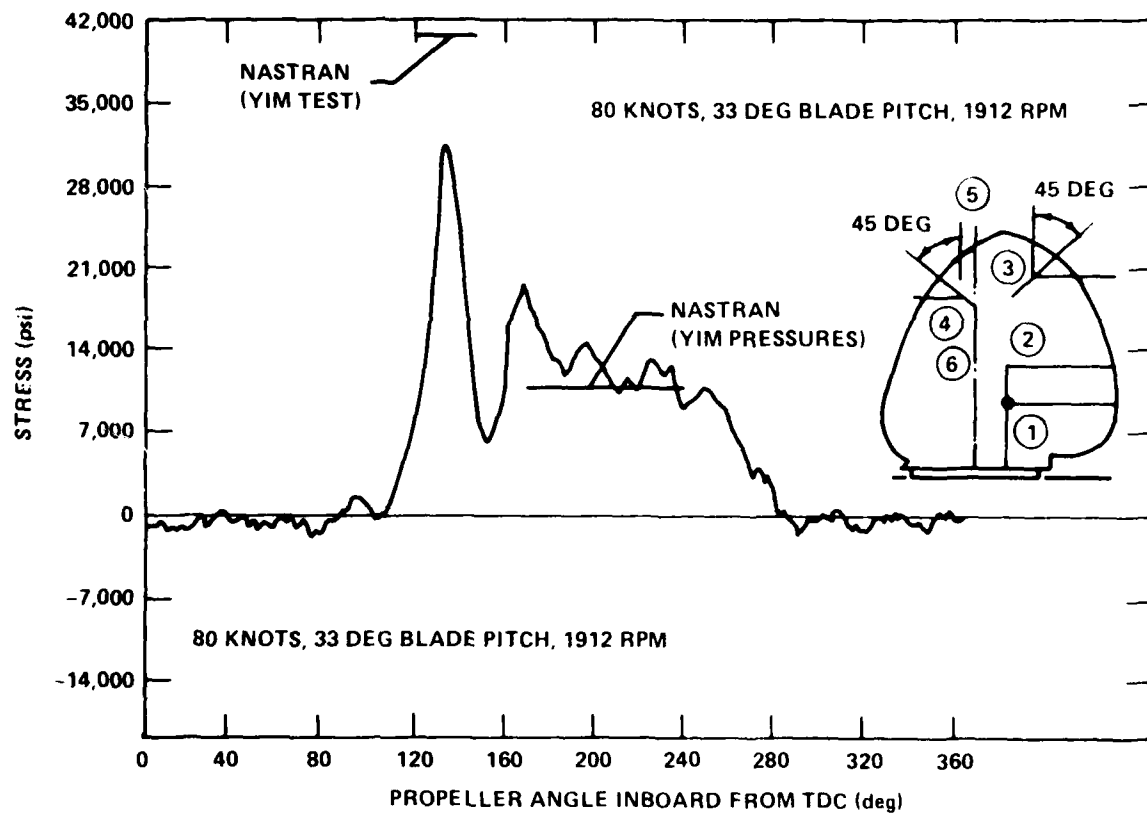


Figure 13 - Experimentally Determined Radial Stress in  
SES-100B Propeller Blade at Gage 1  
©(From Reference 5)

TABLE 1 - CALCULATED NATURAL FREQUENCIES OF P3604 PROPELLER BLADE

Vibration Mode, N	Calculated Frequencies		Frequency Ratio, $\frac{\text{in Water}}{\text{in Air}}$
	In Air	In Water	
1	461	225	0.49
2	1228	671	0.55
3	1680	774	0.46
4	2397	1171	0.49
5	2613	1315	0.50

TABLE 2 - NATURAL FREQUENCIES OF SES-100B PROPELLER BLADE

Vibration Mode, N	Calculated Frequencies			
	In Air	In Water		
		Stage 1	Stage 2	Stage 3
1	624	524	425	420
2	1399	1037	924	916
3	1679	1316	1206	1158
4	2488	1893	1644	1581
5	2612	2045	1815	1797

## APPENDIX - INPUT DATA PREPARATION

Input required for the vibration and transient response analyses in this report will be described using the SES-100B calculations as examples. Inputs described will be those required for the fluid H and L matrix runs, propeller vibration runs in water, and propeller transient response runs, with progressive submergence of the blade. The fluid matrix is the same for either the vibration or the transient response runs.

NASTRAN input decks consist of control cards, an Executive Control deck, a Case Control deck, and a Bulk Data deck. Formats for all cards used here are defined in the NASTRAN User's Manual. The DMAP ALTER instructions contained in the Executive Control Deck and the checkpoint dictionaries apply only to NASTRAN Level 17.

### FLUID MATRIX CALCULATION

To obtain a series of fluid H and L matrices, one for each stage of submersion, one static stress computer run is made for each stage. These are basically static stress (Rigid Format 1) runs, utilizing CIHEX2 elements. For convenience, all grid points should be assigned numbers higher than those to be assigned to any grid points of the propeller. The element and grid point data are assembled in the usual way, with the following exceptions and notations.

1. All degrees of freedom of all grid points on the outer boundary, except for those on that part of the fluid-structure interface surface that are to be in contact with the propeller during the current stage, are constrained with SPC cards.
2. All but one translational degree of freedom (components 1, 2, or 3) of all other grid points are constrained.

3. Material properties are input on a MAT1 card. The value of the shear modulus entered is the reciprocal of the mass density of water,  $1/\rho$ , for the present case in which water contacts only one side of the blade. Young's modulus is a very large factor, say  $10^{20}$ , times the shear modulus. No value is input for Poisson's ratio, so that the NASTRAN program will compute a value.

4. Unit pressure is applied on the element faces of the fluid-structure interface which are to be in contact with the propeller in the present stage. Input is by means of PLOAD3 cards. The unit pressure can be either positive or negative, as the sign will not affect the final result.

5. All grid points in contact with the propeller during this stage are listed on ASET1 cards.

The Executive Control and Case Control decks, and two additional catalog instructions which must be included in the control cards, are shown in Figure A.1. The two instructions identify two permanent files, HMATRIXSTEP1, and LOADSANDTABLES1, which will contain the H matrix and other information, respectively.

For the second and succeeding stages of submersion, the only physical change is that a new set of grid points comes into contact with the propeller blade. This set will generally include all the gridpoints included in the previous stage of submersion. For each succeeding run, then, the grid points newly in contact with the propeller must be added to the set of ASET1 points and removed from the SPC set for which all degrees of freedom are constrained. The element faces newly in contact with the propeller must be added to the set of loaded element faces, and the CATALOG

cards must be changed to assign new names to the H matrix and other data. The names used here for the second step were HMATRIXSTEP2 and LOADSANDTABLES2.

The printout of the "PG" matrix, or list of equivalent forces, is shown in Figure 15. It was necessary to obtain this matrix before constraints were applied in order to obtain all three components for each grid point; consequently, the zeros for all other unloaded components were also printed out. Each group of three non-zero numbers represents the three components of force at a fluid grid point in contact with a propeller grid point. The numbers are given in the order in which the fluid grid points are numbered. These values are to be entered as  $L^T$  matrix terms on DMIT cards on which the matching fluid and propeller interface grid points will also be listed. The procedure for entering these terms on DMIT cards is best understood by examining the example to be presented later.

#### VIBRATION ANALYSIS

The Executive Control and Case Control decks for the vibration analysis of a submerged propeller, and two ATTACH instructions which must be included with the control cards, are given in Figure A.2. The file names on these two cards identify the H matrix and other data which have been created by a previous run. In this example, the names identify the third, or fully-submerged, case. The ALTER routine in the Executive control deck contains two partition (PARTN) instructions, one of which contains the matrix name, PVEG3. That name was arbitrarily chosen to identify a partitioning column matrix of the same name to be input in the bulk data.

The bulk data is set up basically as a propeller vibration run, with the following additions:

1. All fluid points in contact with the propeller (in this fully-submerged case, all fluid-structure interface points) are listed as scalar points on SPOINT cards in this propeller run.

2. Constraints on the zero component of these scalar points are input on SPC cards.

3. Two column matrices, PVECD1 and PVEC3, are input. In this example the total number of unconstrained degrees of freedom is 96x6, or 576 for the propeller, plus 40 for the scalar points, or 616. Dimensions of the two column matrices, therefore, are 1x616. All entries in PVECD1 are zero, and all except the last 40 (assuming the SPOINT numbers are higher than all propeller grid point numbers) of the PVEC3 entries are zero. The remaining 40 entries are 1.0.

4. The  $L^T$  matrix terms are input on DMIG cards. In this case, 40x3 terms are input.

#### TRANSIENT RESPONSE ANALYSIS

The procedures for preparing the additional bulk data input for the vibration analysis are essentially the same as those for the transient response case, which will be illustrated in more detail.

The Executive Control, Case Control, and Bulk Data decks, and the four additional control cards, for the first stage of submersion of the transient response case are shown in Figure A.4. Of the four control cards, the two ATTACH instructions retrieve the appropriate H matrix for this step, as in the vibration calculation. The REQUEST and CATALOG instructions effect the storage of the checkpoint file named SUBSTP1, required for the restart. The bulk data input consists of the same data as for a straightforward transient response analysis, and additional SPOINT, SPC, DMIG, and

DMI data similar to that for the vibration in water case. The following comments apply to the additional data;

1. All fluid grid points to come into contact with the propeller during the course of the analysis (not just those in contact in the current stage of submersion) must be listed as scalar points on SPOINT cards, and also on SPC cards because scalar points cannot be added after solution of the problem has begun.

2. PVECD1 and PVEC1 matrices have the same dimensions for all stages, in this example  $1 \times 616$ . The number of "1.0" terms in PVEC1, however, in this case 18, must be equal to the number of fluid points in contact with the propeller for the current stage, and the placement of these terms within the "scalar point section" of the PVEC1 column (the last 40 numbers) must correspond to the positions of the 18 contact points within the "scalar point section." All degrees of freedom of propeller grid points and scalar points are represented in the PVEC1 column in numerical order. In this example the fluid points were numbered so that the portions of the blade with the highest numbered points contact the water first; thus any "1.0" entries in PVEC1, or PVEC2, etc., are the last terms in the column.

3. The  $L^T$  matrix input by DMIG cards for this stage was made up from the corresponding "PG" matrix printout from the first stage fluid run, given in Figure A.2. The current run is terminated when the time covered by the TSTEP card, that is, number of steps times length of each step (in this case  $0.9095 \times 10^{-3}$  seconds), has elapsed.

To continue the analysis for the second stage of submersion, a restart run is carried out, with the following changes to the deck:

1. The two ATTACH instructions and the CATALOG instruction described for the first run are replaced with the following control cards:

```
ATTACH,OPTP,SUBSTP1, ID=CSRV.  
ATTACH,INPT,HMATRIXSTEP2, ID=CSRV .  
ATTACH,UT1, LOADSANDTABLES2, ID=CSRV .  
CATALOG,NPTP,SUBSTP2, ID=CSRV .
```

2. The checkpoint dictionary produced by the previous run is added to the Executive Control deck. Also, PVEC1, which appears in one of the PARTN instructions, is changed to PVEC2. The following lines are added to the previous ALTER routine and left for the remaining restart runs:

```
ALTER 143,143  
CHKPNT K2PP, K2DD,M2DD,B2DD,MDD,KDD $  
ALTER 159,159
```

3. The TSTEP card, TSTEP=21, in the Case Control deck, is replaced with TSTEP=22.

4. The Bulk Data deck consists of the following cards:

- a. A delete (/) card which eliminates the previous DMIG cards.
- b. MIG cards, which represent the  $L^T$  matrix for stage two.
- c. DMI cards for a new column matrix, PVEC2. Dimensions are the same as for PVEC1, but the number of "1.0" terms is changed to represent the new set of points in contact with the propeller. In this case, the last 28 terms are now 1.0.
- d. A new TSTEP Bulk Data card, identified as TSTEP number 22, to correspond to the Case Control TSTEP card. This card should contain the correct number of time steps so that the total time defined will just cover the current stage of

submersion. In this second stage, 28 steps were used.

To continue with the third and any succeeding steps, the procedures for the second stage are followed. The REQUEST and CATALOG control cards and the CHKPNT Executive Control deck card are not required in the final run.

CATALOG,INPT,HMATRIXSTEP1, ID=CSRV.  
CATALOG,UT1,LOADSANDTARI,ES1, ID=CSRV.

N A S T R A N   E X E C U T I V E   C O N T R O L   D E C K

IO SES PROPELLER FLUID IDEALIZATION  
APP DISPLACEMENT  
SOL 1,0  
DIAG 1,8,14,22  
TIME 60  
ALTER 97  
MATPRN KAA,,,//\$/  
OUTPUT1 ,,,//C,N,-1 \$  
OUTPUT1 KAA,,,// \$  
JUMP LBL7 \$  
ALTER 112  
MATPRN PG,ASET,,,// \$  
OUTPUT2 PG,EQEKIN,ASET,,,//C,N,0/C,N,11\$  
TABPT EQEXIN,,,// \$  
JUMP MEL \$  
ALTER 141  
LABEL MEL \$  
EQUIV PG,PGG \$  
ALTER 143  
JUMP LBL0FP \$  
ALTER 165  
JUMP FINIS \$  
ENDALTER  
CEND

C A S E   C O N T R O L   D E C K

TITLE = SES PROPELLER FLUID  
SUBTITLE = ADDED MASS TERMS  
SPC = 11  
LOAD = 1  
DISPLACEMENT = ALL  
MAXLINES = 500000  
BEGIN BULK

Figure A.1 - Fluid Run Partial Input

SES PROPELLER FLUID  
ADDED MASS TERMS

```
WATRIX PG {CINO NAME 101 } IS A REAL 1 COLUMN X 1654 304 RECINT MATRIX
```

THE NUMBER OF NON-ZERO WORDS IN THE LONGEST RECORD  
THE DENSITY OF THIS MATRIX IS 517 PERCENT.

Figure A.2 = Matrix PC of Equivalent Nodal Forces

ATTACH,INPT,HMATRIXSTEP3, ID=CSRV.  
ATTACH,UT1,LOADSANDTABLES3, ID=CSRV.

N A S T R A N E X E C U T I V E C O N T R O L D E C K

ID VIBRATION SES PROP IN WATER  
APP DISPLACEMENT  
SOL 3,C  
DIAG 1,4,14,22  
TIME 50  
ALTER 53  
OPD DYNAMICS,GPL,SIL,USET/GPLD,SILD,USETD, , , , , , EED,EQDYN/V,N,  
LUSET/V,N,LUSETD/V,N,NOTFL/V,N,NOFLT/V,N,NOPSDL/V,N,NOFR/V,  
N,NONLFT/V,N,NOTRL/V,N,NOEED/C,N,/V,N,NOUE \$  
SAVE NOEED,LUSETD \$  
MTRXIN CASECU,MATPOOL,FQDYN,,/K2DPP,M2DPP,B2PP/V,N,LUSETD/V,  
N,NOK2DPP/V,N,NOM2DPP/V,N,NOB2PP \$  
PARTN K2DPP,,PVEC3/UNUSED,ATMAT,,/C,N,1 \$  
INPUTT1 /,,,/C,N,-1 \$  
INPUTT1 /HMAT,,,/ \$  
SOLVE HMAT,ATMAT/HIAT/C,N,1 \$  
MPYAD ATMAT,HIAT,MGG/MGGTEM/C,N,1 \$  
PARTN MGGTEM,PVEC1,/MGGNEW,,,/C,N,-1/C,N,2/C,N,6 \$  
PARAM //C,N,MPY/V,N,PDUM/C,N,1/C,N,-1 \$  
EQUIV MGGNEW,MGG/PDUM \$  
JUMP DICK \$  
MATPRN MGGNEW,MGG,,,// \$  
LABEL DICK \$  
ALTER 9F,97  
ENDALTER  
CHKPNT YES  
CEND

L A S E C O N T R O L D E C K

TITLE=SES PROP VIBRATION  
SUBTITLE = PARTIALLY SUBMERGED PROPELLER  
LABEL = INVERSE POWER METHOD  
ECHO = BOTH  
K2PP = STFF  
MFTHOD=41  
SPC=10  
DISPLACEMENT = ALL  
MAXLINES = 5000  
BEGIN BULK

Figure A.3 - Propeller Vibration Run Partial Input

Figure A.4 - Propeller Transient Response Run Input for Stage 1

```
REQUEST,NPTP,*PF.  
ATTACH,INPT,HMATRIXSTEP1, ID=CSRV.  
ATTACH,UT1,LOADSANDTABLEFS1, ID=CSRV.  
CATALOG,NPTP,SUBSTP1, ID=CSRV.
```

N A S T R A N   E X E C U T I V E   C O N T R O L   D E C K   E C H O

```
TO TRANSIENT RESPONSE OF SES PROPELLER IN WATER  
APP DISPLACEMENT  
SOL 9,0  
OTAG 1,8,14,22  
TTME 60  
ALTER 72  
DPD DYNAMICS,CPL,STL,USET/GPLD,SILD,USETD,TFPUOL,DLT,,,NLFT,TRL,,  
EQDYN/V,N,LUSET//V,N,LUSETD/V,N,NOTFL/V,N,NOBLT/V,N,NOPSL/V,  
N,NOFRL/V,N,NONLFT/V,N,NOTRL/V,N,NOEED/C,N,/V,N,NOUE $  
SAVE LUSETB,NOBLT,NONLFT,NOTRL,NOUE $  
MTRYIN CASECC,MATPOOL,EQDYN,,TFPOOL/K2DPP,M2DPP,B2PP/V,N,LUSFTD/V,N,  
NOK2DPP/V,N,NOM2DPP/V,N,NOB2PP $  
SAVF NOK2DPP,NOM2DPP,NOB2PP $  
PARTM K2DPP,,PVEC1/UNUSED,ATMAT,,/C,N,1 $  
INPUTT1 7,,,./C,N,-1 $  
TNPPUTT1 /HMAT,,,./ $  
SOLVE HMAT,ATMAT/HIAT/C,N,1 $  
MPYAD ATMAT,HIAT,MGG/MGGTEM/C,N,1 $  
PARTN MGGTEM,PVEC1,/MGGNEW,,,/C,N,-1/C,N,2/C,N,6 $  
EQUTV MGGNEW,MGG $  
JIMF DICK $  
MATPRN MGGNEW,MGG,,,// $  
LABEL DICK $  
ALTER 114,115  
ALTER 128,129  
ENDALTER  
CHKPNT YES  
CEND
```

Figure A.4 (Continued)

SES PROPELLER DYNAMIC RESPONSE  
PARTIALLY SUBMERGED PROPELLER  
DIRECT TRANSIENT RESPONSE

C A S E   C O N T R O L   D E C K   E C H O

CARD  
COUNT  
1           TITLE = SES PROPELLER DYNAMIC RESPONSE  
2           SUBTITLE = PARTIALLY SUBMERGED PROPELLER  
3           LABEL = DIRECT TRANSIENT RESPONSE  
4           ECHO = BOTH  
5           DLOAD = 10  
6           TSTEP = 21  
7           K2PP = STFF  
8           SET 5 = 2  
9           ELSTRESS = 5  
10          SPC = 10  
11          DISPLACEMENT=ALL  
12          MAXLINES = 500000  
13          BEGIN BULK

Figure A.4 (Continued)

SFC PROPELLER DYNAMIC RESPONSE  
PARTIALLY SUBMERSED PROPELLER  
DIRECT transient RESPONSE

TURN	RIGHT	1	2	3	4	5	6	7	8	9	10
1-	RTHEY	1	38	6	7	8	5	3	2	11	
2-	+11	1	4	21	22	20	19	32	33	+21	
3-	+21	34	31	29	28	27	30				
4-	RTHEX2	2	30	11	12	13	10	8	7	+12	
5-	+12	6	9	23	24	22	21	37	36	+22	
6-	+22	30	36	34	33	32	35				
7-	RTHEY2	3	38	16	17	18	15	13	12	+13	
8-	+13	11	14	25	26	24	23	42	43	+23	
9-	+23	44	41	39	38	37	40				
10-	RTHEY2	4	30	32	33	34	31	29	28	+14	
11-	+14	27	30	47	48	46	45	58	59	+24	
12-	+24	60	57	55	56	53	56				
13-	RTHEY2	5	30	37	38	39	36	34	33	+15	
14-	+15	37	35	49	50	48	47	63	64	+25	
15-	+25	62	60	59	58	61					
16-	RTHEY2	6	30	42	43	44	41	39	38	+16	
17-	+16	37	40	51	52	50	49	68	69	+26	
18-	+26	70	67	65	64	63	66				
19-	CIMEX2	7	30	58	59	50	57	55	54	+17	
20-	+17	53	56	73	74	72	71	86	85	+27	
21-	+27	86	87	81	80	79	82				
22-	CIMEX2	8	30	63	64	65	62	60	59	+18	
23-	+18	58	61	75	76	74	73	80	80	+28	
24-	+28	91	88	86	85	84	87				
25-	CTHEX2	9	78	68	69	70	67	65	64	+19	
26-	+19	63	66	77	74	76	75	96	95	+29	
27-	+29	95	93	91	90	89	92				
28-	DAREA	121	21	1	6.20	21					
29-	DAREA	121	21	3	6.60						
30-	DAREA	123	23	1	10.70	23					
31-	DAREA	123	23	3	9.40						
32-	DAREA	167	47	1	9.32	47					
33-	DAREA	147	47	3	14.91						
34-	DAREA	149	69	1	11.39	49					
35-	DAREA	149	49	3	13.97						
36-	DAREA	177	73	1	5.57	73					
37-	DAREA	173	73	3	9.77						
38-	DAREA	175	75	1	6.23	75					
39-	DAREA	175	75	3	6.53						
40-	DLOA	19	1.0	1.0	2.0	1.0	30	1.0	40	+PL1	
41-	+DL1	1.0	1.0	1.0	1.0	1.0	70				
42-	DM	1	2	1	1	1		616	1		
43-	DM1	1	1	1	1	1					
44-	DM1	1	2	1	1	1		616	1		
45-	DW1	1	1	1	1	1					
46-	+PV11	1.0	1.0	1.0	1.0	1.0					
47-	+PV12	1.0	1.0	1.0	1.0	1.0					
48-	MTG	0	2	1	1	1					
49-	MTG	53	1	235							
50-	MTG	54	2								

Figure A.4 (Continued)

CFD FOWLER DYNAMIC RESPONSE  
OBTAINING COUNTER ROTATION  
REPORT PRESENT EFFECTIVE

		SORTED BULK DATA ECHO									
POINT	TIME	1	2	3	4	5	6	7	8	9	10
51-	0.000	STFF	53	235	3980						
51-	0.000	STFF	56	240	9293						
52-	0.000	STFF	56	240	1753						
53-	0.000	STFF	56	240	1760						
54-	0.000	STFF	56	240	6694						
55-	0.000	STFF	56	243	0311						
56-	0.000	STFF	59	243	11226						
57-	0.000	STFF	59	243	2.8E-6						
58-	0.000	STFF	61	243	0195						
59-	0.000	STFF	61	243	3.2924						
60-	0.000	STFF	61	243	6957						
61-	0.000	STFF	63	251	08556						
62-	0.000	STFF	63	251	0993						
63-	0.000	STFF	63	251	0.8671						
64-	0.000	STFF	65	256	2367						
65-	0.000	STFF	66	256	1.407						
66-	0.000	STFF	66	256	2255						
67-	0.000	STFF	66	256	0.396						
68-	0.000	STFF	68	259	3034						
69-	0.000	STFF	68	259	7647						
70-	0.000	STFF	71	272	1266						
71-	0.000	STFF	71	272	1.490						
72-	0.000	STFF	73	275	3.014						
73-	0.000	STFF	73	275	220						
74-	0.000	STFF	73	275	5.249						
75-	0.000	STFF	74	275	3.070						
76-	0.000	STFF	75	274	213						
77-	0.000	STFF	75	274	4.5220						
78-	0.000	STFF	75	274	7459						
79-	0.000	STFF	77	281	195						
80-	0.000	STFF	77	281	1.048						
81-	0.000	STFF	77	281	2539						
82-	0.000	STFF	79	284	0495						
83-	0.000	STFF	79	284	0.0276						
84-	0.000	STFF	79	284	1.0759						
85-	0.000	STFF	81	289	7728						
86-	0.000	STFF	81	289	0.0827						
87-	0.000	STFF	81	289	0.181						
88-	0.000	STFF	81	289	3.4611						
89-	0.000	STFF	84	292	7543						
90-	0.000	STFF	84	292	0.085						
91-	0.000	STFF	87	297	1.1960						
92-	0.000	STFF	87	297	0.7552						
93-	0.000	STFF	87	297	1586						
94-	0.000	STFF	92	305	0.0591						
95-	0.000	STFF	92	305	2980						
96-	0.000	STFF	94	304							

**SFC PROPELLER DYNAMIC RESPONSE  
PARTIALLY SUPERFUGER PROPELLER**  
**DIRECT TRANSIENT RESPONSE**

Figure A.4 (Continued)

S O R T E D   B U L K   D A T A   E C H O											
C A R M		I M T R		S T E F F		I M T R		S T E F F		I M T R	
1	1	1	2	2	3	3	4	4	5	5	6
2	2	2	3	3	4	4	5	5	6	6	7
3	3	3	4	4	5	5	6	6	7	7	8
4	4	4	5	5	6	6	7	7	8	8	9
5	5	5	6	6	7	7	8	8	9	9	10
6	6	6	7	7	8	8	9	9	10	10	10
7	7	7	8	8	9	9	10	10	10	10	10
8	8	8	9	9	10	10	10	10	10	10	10
9	9	9	10	10	10	10	10	10	10	10	10
10	10	10	10	10	10	10	10	10	10	10	10
11	11	11	11	11	11	11	11	11	11	11	11
12	12	12	12	12	12	12	12	12	12	12	12
13	13	13	13	13	13	13	13	13	13	13	13
14	14	14	14	14	14	14	14	14	14	14	14
15	15	15	15	15	15	15	15	15	15	15	15
16	16	16	16	16	16	16	16	16	16	16	16
17	17	17	17	17	17	17	17	17	17	17	17
18	18	18	18	18	18	18	18	18	18	18	18
19	19	19	19	19	19	19	19	19	19	19	19
20	20	20	20	20	20	20	20	20	20	20	20
21	21	21	21	21	21	21	21	21	21	21	21
22	22	22	22	22	22	22	22	22	22	22	22
23	23	23	23	23	23	23	23	23	23	23	23
24	24	24	24	24	24	24	24	24	24	24	24
25	25	25	25	25	25	25	25	25	25	25	25
26	26	26	26	26	26	26	26	26	26	26	26
27	27	27	27	27	27	27	27	27	27	27	27
28	28	28	28	28	28	28	28	28	28	28	28
29	29	29	29	29	29	29	29	29	29	29	29
30	30	30	30	30	30	30	30	30	30	30	30
31	31	31	31	31	31	31	31	31	31	31	31
32	32	32	32	32	32	32	32	32	32	32	32
33	33	33	33	33	33	33	33	33	33	33	33
34	34	34	34	34	34	34	34	34	34	34	34
35	35	35	35	35	35	35	35	35	35	35	35
36	36	36	36	36	36	36	36	36	36	36	36
37	37	37	37	37	37	37	37	37	37	37	37
38	38	38	38	38	38	38	38	38	38	38	38
39	39	39	39	39	39	39	39	39	39	39	39
40	40	40	40	40	40	40	40	40	40	40	40
41	41	41	41	41	41	41	41	41	41	41	41
42	42	42	42	42	42	42	42	42	42	42	42
43	43	43	43	43	43	43	43	43	43	43	43
44	44	44	44	44	44	44	44	44	44	44	44
45	45	45	45	45	45	45	45	45	45	45	45
46	46	46	46	46	46	46	46	46	46	46	46
47	47	47	47	47	47	47	47	47	47	47	47

Figure A.4 (Continued)

**RCF PROPULLED MASTERS' RESPONSE  
SOCIALLY SUPPORTED MASTERS' RESPONSE  
TO PERTURBANT RESPONSE**

FACID		S O R T E D   B U L K   C A T A   E C H O									
1	GRIN	4.0	-2.021	6.875	-63.96	6..	6..	6..	6..	6..	6..
151	GRIN	4.0	-1.127	4.425	-0.4123						
152	GRIN	5.0	-7.080	4.425	-0.9710						
153	GRIN	5.0	3.607	2.7	-5.1171						
154	GPIN	5.1	3.593	2.2	-3.1267						
155	GRIN	5.2	-2.738	11.45	1.4487						
156	GRIN	5.3	-2.805	11.45	1.7046						
157	GPIN	5.4	-2.872	11.45	1.1605						
158	GPIN	5.5	-1.463	10.25	1.1280						
159	GRID	5.6	-2.064	10.25	0.7585						
160	GRIN	5.7	-1.045	9.05	-0.8033						
161	GPID	5.8	-1.185	9.05	-0.799						
162	GPIN	5.9	-1.756	9.05	-3.325						
163	GPIN	6.0	-2.351	7.475	-0.394						
164	GRIN	6.1	-0.005	7.475	-0.9903						
165	GRID	6.2	1.486	5.9	-0.7295						
166	GPIN	6.3	1.76	5.9	-0.3113						
167	GRIN	6.4	1.235	5.9	-1.1331						
168	GRIN	6.5	2.570	4.55	-1.0023						
169	GPID	6.6	2.442	4.55	-2.0091						
170	GPID	6.7	3.656	3.2	-2.8750						
171	GPIN	6.8	3.653	3.2	-2.801						
172	GRIN	6.9	3.649	3.2	-2.8851						
173	GPIN	7.0	-1.835	11.45	-0.9761						
174	GRIN	7.1	-1.946	11.615	-7558						
175	GPIN	7.2	-0.190	10.0	.2206						
176	GRIN	7.3	-0.211	10.0	-0.0105						
177	GRID	7.4	2.185	6.55	-1.2028						
178	GPID	7.5	2.059	6.55	-1.4081						
179	GPIN	7.6	3.560	4.2	-2.5836						
180	GRIN	7.7	3.553	4.2	-2.5931						
181	GRIN	7.8	-0.960	11.78	.5034						
182	GRIN	7.9	-0.961	11.78	.4277						
183	GPID	8.0	-0.937	11.78	.3511						
184	GRIN	8.1	-0.074	11.365	.0687						
185	GRIN	8.2	-0.121	11.165	-0.0112						
186	GPIN	8.3	-7.766	10.95	-0.1661						
187	GPIN	8.4	-7.750	10.95	-0.3699						
188	GPID	8.5	-7.773	10.95	-0.3734						
189	GPIN	8.6	2.056	9.219	-1.0774						
190	GPID	8.7	2.049	9.219	-1.0774						
191	GPID	8.8	2.049	7.02	-1.6761						
192	GPIN	8.9	2.049	7.02	-1.6761						
193	GPIN	9.0	2.049	7.02	-1.6761						
194	GPIN	9.1	2.049	7.02	-1.6761						
195	GPID	9.2	2.049	7.02	-1.6761						
196	GRIN	9.3	3.179	6.02	-1.9841						
197	GPIN	9.4	3.463	5.07	-2.2921						
198	GPIN	9.5	3.462	5.02	-2.2966						
199	GRIN	9.6	3.456	5.02	-2.5011						
200	GRIN	9.7	3.456	5.02	4.274						

RESPECT TRANSIENT RESENSE  
PREDICTION DYNAMIC PROFILE?

Figure A.4 (Continued)

REFERENCES

1. Everstine, G.C. et al. "The Dynamic Analysis of Submerged Structures," NASTRAN: User's Experiences, NASA TM X-3278 (1975).
2. Zienkiewicz, O.C. and R.E. Newton, "Coupled Vibrations of a Structure Submerged in a Compressible Fluid," Proc. Int. Symp on Finite Element Techniques, Stuttgart, Germany (June 1969).
3. Everstine, G.C., "A NASTRAN Implementation of the Doubly Asymptotic Approximation for a Underwater Shock Response," NASA TM X-3428 (1976).
4. Marcus, M.S., "A Finite Element Method Applied to the Vibration of Submerged Plates," Journal of Ship Research, Vol. 22, No. 2 (June 1978).
5. Allison, J., "Propellers for High Performance Craft," Paper No. 5, 30th Anniversary Spring Meeting of the Gulf Section, SNAME (Mar 1978).
6. Lewis, R., "Helicoidal Propeller Structural Design," Bell Aerospace Analysis Report 7593-902002 (May 1978).
7. Pierson J., "Penetration of Fluid by a Wedge," Stevens Institute of Technology, ETT Report 381 (July 1950).
8. Wang, D.P., "Water Entry and Exit of a Fully Ventilated Foil," Journal of Ship Research, Vol. 21, No. 1 (Mar 1977).

INITIAL DISTRIBUTION

Copies		Copies	
1	CNO, Code 987	1	NAVSHIPYD L.BEACH
1	CHONR, Code 474	1	NAVSHIPYD MARE
1	ONR BOSTON	1	NAVSHIPYD NORVA
1	ONR CHICAGO	1	NAVSHIPYD PEARL
1	ONR LONDON, ENGLAND	1	NAVSHIPYD PHILA
1	ONR PASADENA	1	NAVSHIPYD PTSMH
3	NRL	12	DTIC
	1 2627	1	NSF ENGR DIV LIB
	1 6300	1	DOT LIB
	1 8400	1	SWRI APPLIED MECH REVIEW
1	USNA	1	ASNE
1	NAVPGSCOL LIB	1	SNAME
1	NROTC & NAVADMINU, MIT	1	BELL AEROSPACE TEXTRON (R. Lewis)
1	NSWC WHITE OAK		
2	NOSC		CENTER DISTRIBUTION
	1 Lib		
	1 8142		

		Copies	Code	Name
1	NWC			
11	NAVSEA	1	11	W.M. Ellsworth
	1 05H	1	1151	W. O'Neil
	1 05H1 (A.R. Paladino)	1	15	W.B. Morgan
	1 05R (C.I. Miller)	1	1532	
	1 05R (G. Graves)	1	154	
	1 52 (R.J. Cauley)	1	1542	B. Yim
	1 52P (Peterson)	1	1544	R. Cumming
	1 521 (F. Welling)	1	1544	R. Boswell
	1 524 (R.M. Petros)	1	1544	E. Caster
	1 PMS-300			
	1 PMS-304			
	1 PMS-304.32			
1	NAVSHIPYD BREM	1	1552	T.E. Brockett
1	NAVSHIPYD CHASN	1	1556	P. Besch
		1	17	W.W. Murray

## CENTER DISTRIBUTION (Continued)

Copies	Code	Name
1	1702	
2	1706s	C. Richardson
1	172	Krenzke
1	1720.1	Kiernan
1	1720.2	Hom
1	1720.3	Jones
1	1720.4	Wiggs
1	1720.5	McDevitt
10	1720.6	Rockwell
1	173	
1	174	
1	177	
1	18	G.H. Gleissner
1	184	J. Schot
10	1844	S. Dhir
1	1905.1	W. Blake
1	1965	Y. Liu
1	1965	J.E. Brooks
1	2740	Y.F. Wang
10	5211.1	Reports Distribution
1	522.1	Enclass Lib (C)
1	522.2	Enclass Lib (A)

**DTNSRDC ISSUES THREE TYPES OF REPORTS**

- 1. DTNSRDC REPORTS, A FORMAL SERIES, CONTAIN INFORMATION OF PERMANENT TECHNICAL VALUE. THEY CARRY A CONSECUTIVE NUMERICAL IDENTIFICATION REGARDLESS OF THEIR CLASSIFICATION OR THE ORIGINATING DEPARTMENT.**
- 2. DEPARTMENTAL REPORTS, A SEMIFORMAL SERIES, CONTAIN INFORMATION OF A PRELIMINARY, TEMPORARY, OR PROPRIETARY NATURE OR OF LIMITED INTEREST OR SIGNIFICANCE. THEY CARRY A DEPARTMENTAL ALPHANUMERICAL IDENTIFICATION.**
- 3. TECHNICAL MEMORANDA, AN INFORMAL SERIES, CONTAIN TECHNICAL DOCUMENTATION OF LIMITED USE AND INTEREST. THEY ARE PRIMARILY WORKING PAPERS INTENDED FOR INTERNAL USE. THEY CARRY AN IDENTIFYING NUMBER WHICH INDICATES THEIR TYPE AND THE NUMERICAL CODE OF THE ORIGINATING DEPARTMENT. ANY DISTRIBUTION OUTSIDE DTNSRDC MUST BE APPROVED BY THE HEAD OF THE ORIGINATING DEPARTMENT ON A CASE-BY-CASE BASIS.**

